

Acoustical Direction Finder

Submitted By:

Mohammad Sami Ahmad Zouher Mnl Rasoul Al-Ayoubi

Mohammad Mamoun Al-Shaar

Mohammad Nebras Mohammad Yasser Mresh

Tasnim Kamal Al-Asali

Randa Mohammad Hamzeh

Under the supervision of:

Prof.Dr.Eng. Samawal Al-Hakeem

Prof.Dr.Eng. Ahmad Al-Najjar

A senior Project Presented to the Faculty of Computer Informatics and Engineering
in Partial Fulfillment of the Requirements for the Degree of Bachelor of Engineering in
Communications and Networking
All Copyrights reserved for SPU University©

2015/2016

Acoustical Direction Finder

Submitted By:

Mohammad Sami Ahmad Zouher MnlA Rasoul Al-Ayoubi

Mohammad Mamoun Al-Shaar

Mohammad Nebras Mohammad Yasser Mresh

Tasnim Kamal Al-Asali

Randa Mohammad Hamzeh

Under The Supervision Of:

Prof.Dr.Eng. Samawal Al-Hakeem

Prof.Dr.Eng. Ahmad Al-Najjar

A senior Project Presented to the Faculty of Computer Informatics and Engineering
in Partial Fulfillment of the Requirements for the Degree of Bachelor of Engineering in
Communications and Networking

Acknowledgements

*Praise be to **ALLAH**, the beneficent the merciful*

*Praise be to **Allah** for the blessing of mind ...*

*Praise be to **Allah** for the blessing of love ...*

*Praise be to **Allah** for his uncountable blessings, and guidance.*

*To Our homeland **Syria**, the cradle of civilizations...*

*To the **martyrs** who sacrificed their lives for the redemption for
homeland...*

*To the **people** who watch over our beloved country's safety and
security....*

*Deepest gratitude and appreciation to those who contributed to the
completion of this work*

Dedication

To the source of love and care ...

To the person who fears over me ...

To the person who prays for me day and night

Mom,

To the teacher of morality ...

To the person who gives me power ...

To the person who sacrificed everything to get me where I am ...

Dad,

To the special people who brings out the best of me ...

To the people who stood by me all my life ...

To the people who pushed me to be better ...

Sisters & Brothers,

To all my family, the symbol of love and giving,

Family,

To the people am proud to have in my life ...

Best friends

Along with all hard working and respected

Teachers,

Abstract

The location of an acoustic source can be estimated by measuring an acoustic direction of incidence and the exact location (range difference) can also be estimated. Methods for determining the direction of incidence based on sound intensity, the phase of cross-spectral functions, and cross-correlation functions are available. In this current work, we implement the cross correlation and GCC_phat methods. Direction of arrival (DOA) estimation using microphone arrays is to use the phase information present in signals from microphones that are spatially separated. For any pair of microphones, the surface on which the time difference of arrival (TDOA) is constant is a hyperboloid of two sheets. Acoustic source localization algorithms typically exploit this fact by grouping all microphones into pairs, estimating the TDOA of each pair, and then finding the point where all associated hyperboloids most nearly intersect. We use the optimum estimator (Chan method) to localize the acoustic source position in 2-dimensional space have been successfully located.

Contents

Abstract	5
List of Abbreviations	6
List of figures	9
Chapter 1: Introduction	
1.1. Introduction.....	11
1.2. History of audio gunshot detection systems.....	11
1.3. Direction of Arrival estimation.....	12
1.4. Acoustic Source Localization.....	13
Chapter 2: Acoustical Characteristics of Gunshot	
2.1. Introduction.....	15
2.2. Muzzle blast.....	15
2.3. Supersonic projectile.....	16
2.4. Mechanical action.....	19
2.5. Surface vibration.....	19
2.6. Example Gunshot Characteristics.....	20
Chapter 3: Wireless Positioning System	
3.1. Introduction.....	23
3.2. Basic methods used in positioning systems.....	24
3.2.1. TOA Estimation.....	24
3.2.2. Time Difference Of Arrival (TDOA) Estimation.....	25
3.2.3. DOA Estimation.....	28
3.2.4. RSSI.....	28
3.3. Acoustic source localization.....	29
Chapter 4: Position Location Estimation	
4.1. Direction of Arrival Estimation.....	30
4.2. Time Difference Of Arrival (TDOA).....	30
4.3. Restrictions on the microphones array geometry.....	31
4.4. Conventional DOA methods.....	33
4.4.1. Cross-correlation.....	33
4.4.2. Generalized Cross-correlation.....	34
4.4.3. Eigenvalue Decomposition (ED) Method.....	34
4.5. Hyperbolic position location.....	36
4.5.1. Localization Algorithm.....	37

Chapter 5: Practical Result	
5.1. Introduction.....	41
5.2. GUI Interface.....	41
5.3. Simulation Result.....	43
5.3.1. Direction of arrival.....	43
5.3.2. Hyperbolic position location.....	46
5.4. DOA Circuit.....	48
5.4.1. Basic components.....	48
5.4.2. System workflow.....	50
5.4.3 Microcontroller programming.....	51
Conclusion	54
Appendixes	
Appendix A	55
Appendix B	58
References	60

List of Abbreviations

DOA	Direction Of Arrival
GCC	Generalized Cross Correlation
GCC-PHAT	GCC-Phase Transform
TDE	Time Delay Estimation
TDOA	Time Difference Of Arrivals
GPSs	Global Positioning Systems
LPS	Local Positioning System
INS	Inertial Navigation System
RFID	Radio Frequency Identification
WLPS	Wireless Local Positioning Systems
TCAS	Traffic alert and Collision Avoidance Systems
TOA	Time Of Arrival
RF	Radio Frequency
RSS	Received Signal Strength
ED	Eigenvalue Decomposition
LMS	Least Mean Square
PL	Position Location
LS	Least Squares

Table of Figures

Figure (1.1) : Sound Ranging Diagram.....	12
Figure(1.2) : A two stage algorithm for sound source localization.....	14
Figure (2.1) : Supersonic bullet shock wave description.....	17
Figure (2.2) : Shock wave recording (“N” wave).....	18
Figure (2.3) : Shock wave ground reflection (elevation view, no scale, bullet into page).....	18
Figure (2.4) : Shock wave front for NATO FNM 83-23 bullet (2750 ft/sec at muzzle, 1980 ft/sec at 1400 feet down range).....	19
Figure (2.5) : Two-channel gunshot recording, M=2.54, oblique trajectory toward the microphones.....	20
Figure (2.6) : Two-channel gunshot recording, M=2.54, perpendicular trajectory, 8 meter offset.....	21
Figure (2.7) : Two-channel gunshot recording, M=2.54, perpendicular trajectory, <1 meter offset.....	22
Figure (2.8) : Two-channel gunshot recording, M=2.54, opposing trajectory (muzzle pointed away from microphones).....	22
Figure. (3.1) : Positioning system classification.....	23
Figure (3.2) : (a) Operation of TOA and RSSI, (b) operation of TDOA, (c) comparison of TOA and TDOA calculations, and (d) operation of DOA.....	27
Figure (4.1) : Schematic depicting the signal receiving time and TDOA.....	31
Figure (4.2) : Two-element microphone array.....	32
Figure (5.1) : Gun finder GUI interface simulator.....	42
Figure (5.2) : The muzzle blast of gun sound used in simulation.....	43
Figure (5.3) : Cross Correlation between microphones signals.....	44
Figure (5.4) : First case simulation result.....	45
Figure (5.5) : DOA for Target in (-1, 6), Mics in (-3, 2), (1, 0), GCC_Phats Estimation.....	45
Figure (5.6) : Hyperbolic position location for Target in (4, 7), Mics in (1, 0), (-1, 0), (0, 1), (0, -1).....	46
Figure (5.7) : Hyperbolic position location for Target in (4, 7), Mics in (1, 0), (-1, 0), (0, 1), (0, -1) with uncertainty in Mics locations.....	47
Figure (5.8) : Hyperbolic position location with 8 Mics, and uncertainty in Mics locations...	47
Figure (5.9) : Atmega8 microcontroller pin configuration.....	48
Figure (5.10) : Gun finder direction circuit schematic.....	49
Figure (5.11) : LM358 internal block diagram.....	50
Figure (5.12) : Gun finder block diagram.....	50
Figure (5.13) : flowchart of microcontroller program.....	51
Figure (5.14) : acoustical direction finding (gun finder) circuit front.....	52
Figure (5.15) : acoustical direction finding (gun finder) circuit back.....	52
Figure (5.16) : Power supply circuit.....	53

Chapter 1

Introduction

1.1. Introduction :

Localization of a point-source is not a new problem, and has been widely studied, especially in the fields of radar and acoustics. Acoustic point-source localization of a sound has numerous applications, from voice tracking to beam steering. Specifically, identifying the location of a gunshot is a useful tool for law enforcement. Having sensor systems installed in high-traffic areas can give early warning of a crime in progress and increase the available information at the scene of a crime.

Gunshot detection and localization system provides information for law enforcers in two regards: it identifies possible gunshot events based on audio information acquired by microphones and interpreted by algorithmic processing, and it also provides the perceived location of the sound source. The system is semi-automatic, which is to say, it operates largely by automated computer programming but still requires human interface to complete its task as designed. Installed systems passively “listen” for specific audio characteristics and alert operators of potential detected gunshot events, but the decision to include or exclude an audio event as a gunshot (and requiring response at the scene) still belongs to a human at the controls.

1.2. History of audio gunshot detection systems :

The origins of many technological advances are often traced back to innovations in different fields, later made applicable through simple redesign. Modern-day gunshot detection systems share similar roots.

The onset of World War I brought about a technique known as “sound ranging,” which provides information regarding the coordinates of artillery weaponry. Developed by William Lawrence Bragg, a British military officer and physicist, initial sound ranging techniques involved arrays of microphones carefully placed in the field of battle to detect sound events from the fired weapons and report back to a monitor at an operating base, as depicted in Figure (1.1). At times, the resulting information contained valuable clues about the sound events’ origins. Though the technique’s success was less-than-desirable in the early years, nations from each of the opposing sides made adjustments to the process to find increasingly useful results.

By World War II, most major military players used sound ranging for mortar detection and counter-artillery measures. In particular, British forces and United States Marines made good use of sound ranging in defensive operations. Although sound ranging equipment had been growing more sophisticated and less costly over the years, radar systems and aerial surveillance took over as the primarily-used gun locating methods in military operations. Radar operators were capable of locating large weaponry faster, derived more conclusive data in settings of extreme terrain or overgrown vegetation, equipment could be outfitted on more mobile units for determining the location of airplanes and vehicles as well, and most importantly, radar could operate without waiting for shots fired.

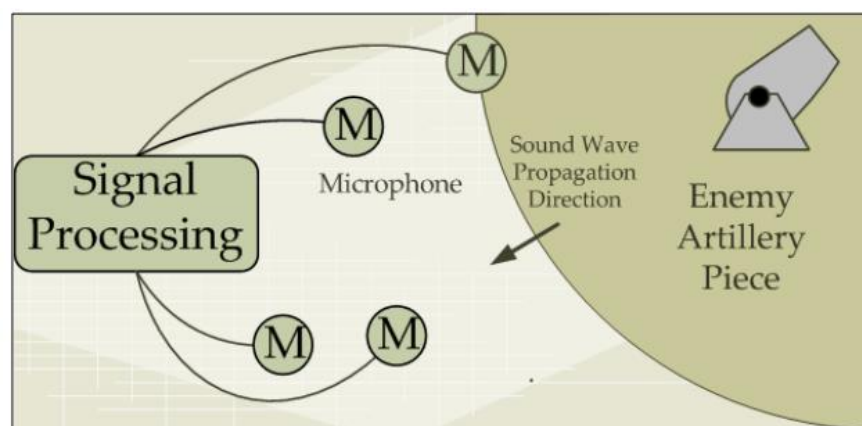


Figure : (1.1) Sound Ranging Diagram

Sound ranging still held a place in combat, but acted mostly as a backup to rapidly expanding radar capabilities. Techniques involving sound ranging for gunfire location receded in popularity until as recently as the 1980s and 1990s. Researchers borrowed sound-ranging techniques from seismologists studying earthquakes and began testing capabilities of detecting small arms activity in urban areas. Organizations such as ShotSpotter Incorporated, now SST Inc., tested detection and localization systems in areas with high crime rates, and US police departments along the Californian Pacific coast began working with the technology to improve incident response time and subsequently help deter future crimes. Meanwhile, the military returned to using gunfire detection and location in combat zones, mainly to assist in evading and countering enemy sniper attacks.

1.3. Direction of Arrival estimation :

Direction of arrival (DOA) estimation using microphone arrays is to use the phase information present in signals picked up by sensors (microphones) that are spatially separated. When the microphones are spatially separated, the acoustic signals arrive at them with differences in time of arrival. From the known array geometry, the Direction of arrival (DOA) of the signal can be obtained from the measured time-delays. The time-delays are estimated for each pair of

microphones in the array. Then the best estimate of the DOA is obtained from time-delays and geometry. Applications like Vehicle Location, vehicle monitoring systems use DOA techniques. Other applications that need a mention are distributed robotics, sensor networks.

Techniques such as the generalized cross correlation (GCC) method, phase transform (GCC-PHAT) are widely used for DOA estimation. The estimated time-delay for a pair of microphones is assumed to be the delay that maximizes the GCC-PHAT function for that pair. Fusing of the pair-wise time delay estimated (TDE's) is usually done in the least squares sense by solving the set of linear equations to minimize the least squared error. The simplicity of the algorithm and the fact that a closed form solution can be obtained has made TDE based methods as a choice for DOA estimation and position location of sound source using microphone arrays. Accuracy of the DOA estimates obtained using the TDE based algorithms depends on various factors. The hardware used for data acquisition, sampling frequency, number of microphones used for data acquisition, and noise present in the signals captured, determine the accuracy of the estimates. Increase in the number of microphones increases the performance of source location estimation. Many of the conventional microphone array techniques for DOA estimates use large number of microphones typically 10 - 40 microphones. This puts a requirement for large number of data acquisition channels, which implies involvement of huge cost. Especially, applications like automatic camera steering uses bulky and huge microphone arrays. This concludes that there is a need for reducing the size and cost involved in time-delay estimation of acoustic source. It also requires multiple data acquisition channels which have to be synchronized in a centralized manner.

1.4. Acoustic Source Localization :

The process of determining the location of an acoustic source relative to some reference frame is known as acoustic source localization. Acoustic source present in the near-field can be localized with knowledge of the time difference of arrivals (TDOAs) measured with pairs of microphones. The speed of sound in the medium in which the acoustic source is Passive acoustic source localization techniques can be used to locate and track an active talker automatically and hence are able to eliminate the human camera operators in current video-conferencing systems. The problem of passively localizing acoustic sources accurately is difficult. Microphone array processing is a rapidly emerging technique and, will play an important role in a practical solution. With continued investigation over the last two decades, the time delay estimation (TDE)-based localization has become the technique of choice.

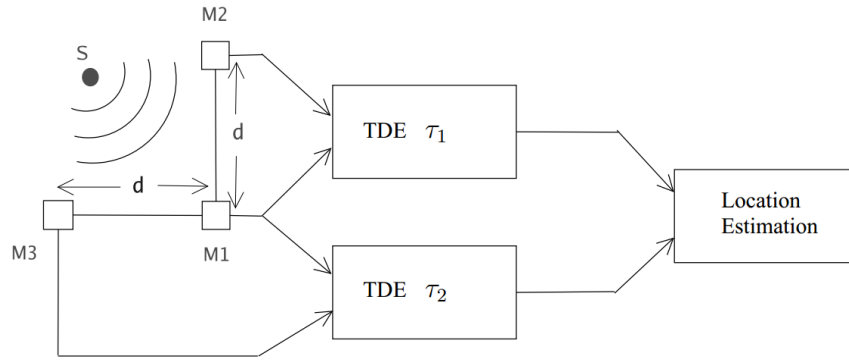


Figure : (1.2) A two stage algorithm for sound source localization.

Most practical acoustic source localization schemes are based on time delay of arrival estimation (TDOA) for the following reasons: such systems are conceptually simple. They are reasonably effective in moderately reverberant environments. Moreover, their low computational complexity makes them well-suited to real-time implementation with several sensors. Time delay of arrival-based source localization is based on a two-step procedure as shown in Figure (1.2)

- The first stage involves estimation of the time difference of arrival (TDOA) between receivers through the use of time delay estimation techniques. The estimated TDOA's are then transformed into range difference measurements between sensors, resulting in a set of nonlinear hyperbolic range difference equations.
- The second stage utilizes efficient algorithms to produce an unambiguous solution to these nonlinear hyperbolic equations. The solution produced by these algorithms result in the estimated position location of the source.

In this thesis, two or more microphones in an array can be used to capture a sound, and then the dissimilarities in the acquired waveforms can yield a point-source location.

Two-stage solutions involve first estimating time delays between microphones and then using the time delays for localization. The critical steps of an implementable two-stage solution are real-time source detection and accurate estimation of time delays between microphones. Source detection requires real-time sampling of multiple inputs in order to obtain relevant data. The detection process is further complicated because a gunshot is broadband, limiting the effectiveness of simple filters.

Time delays estimated with the acquired data must be accurate, a process made difficult by the signal being highly localized in time, which limits the available data and therefore degrades accuracy. Synchronization issues between waveforms can also degrade accuracy, so system-induced delays introduced during the detection and acquisition of data must be compensated for.

Chapter 2

Acoustical Characteristics of Gunshot

2.1. Introduction:

This chapter addresses several practical and theoretical issues encountered in the analysis of gunshot sounds. Gunshot sounds have the potential for tactical detection. Sounds of gunshots can provide information about the gun location, the speed and trajectory of the projectile, and in some cases, the type of firearm and ammunition. However, sounds of gunshots typically contain background noise and reverberation due to the reflecting off and diffracting around nearby surfaces and these effects may limit the reliability of the acoustic estimates.

A variety of commercial and experimental acoustical detection and classification systems designed for gunshot sounds are available. These systems can be intended to detect acoustical “gunshot signatures,” to classify or identify specific firearm types, and to detect and localize snipers. The degree to which a system can achieve satisfactory performance is typically limited by the assumptions required to estimate the firearm and/or projectile behavior based on the available acoustic evidence. Assessing and evaluating acoustic gunshot detection systems requires a thorough understanding of the characteristics of gunshot sounds and the significance of sound wave reflection, absorption, and diffraction from the ground, buildings, and other nearby objects.

2.2. Muzzle blast:

A conventional firearm uses a confined explosive charge to propel the bullet out of the gun barrel. The hot, rapidly expanding gases cause an acoustic muzzle blast to emerge from the barrel. This acoustic disturbance lasts 3-5 milliseconds. The muzzle blast propagates through the air at the speed of sound (e.g., 343 m/s at 20°C) and interacts with the surrounding ground surface, obstacles, temperature, and wind gradients in the air, spherical spreading, and atmospheric absorption. If a recording microphone is located close to the firearm, the direct sound of the muzzle blast is the primary acoustical signal. On the other hand, if the microphone is located at a greater distance from the firearm the direct sound path may be obscured and the received signal will

exhibit propagation effects, multi-path reflections, and reverberation. The blast may also be obscured by barriers and other obstacles blocking the direct path between the firearm and the microphone location.

The muzzle blast is not necessarily a reliable acoustic source for analysis. For most firearms the sound level of the muzzle blast is strongest in the direction the barrel is pointing, and decreases as the off-axis angle increases. Furthermore, some firearms can be equipped with an acoustical suppressor (“silencer”) to alter or reduce the muzzle blast sound level. Suppressors are designed to reduce the audible report (and often the visible explosive flash) of the muzzle blast to reduce the likelihood of detection and/or to prevent hearing damage. Thus, gunshot acoustical detection systems that rely on the muzzle blast must accept the possibility of suppressor use by clandestine individuals.

2.3. Supersonic projectile:

A second source of acoustic information is present if the bullet travels at supersonic speed, $V > c$. The supersonic projectile causes an acoustic shock wave that propagates away from the bullet's path. The shock wave expands as a cone behind the bullet, with the wave front propagating outward at the speed of sound. The shock wave cone has an inner angle, $\theta_M = \arcsine(1/M)$, where $M = V/c$ is the Mach Number. θ_M is referred to as the Mach angle. The shock wave geometry is shown in Figure (2.1). With a very fast bullet, M is large and θ_M becomes small, causing the shock wave to propagate nearly perpendicularly to the bullet's trajectory. For example, a bullet traveling at 3000 feet per second at room temperature has $M = 2.67$, giving $\theta_M = \sim 22^\circ$. On the other hand, if the bullet is only slightly faster than the speed of sound, M is approximately unity, θ_M is nearly 90° , and the shock wave propagates nearly parallel to the bullet's path. If two or more microphones are located at known locations within the path of the shock wave, the time of arrival differences can be used to estimate the shock's propagation direction. Note, however, that determining the bullet's trajectory from the shock propagation vector requires knowledge of the bullet velocity, V . If V is not known, then M and θ_M are also not known, and the bullet's trajectory cannot be determined exactly without additional spatial information.

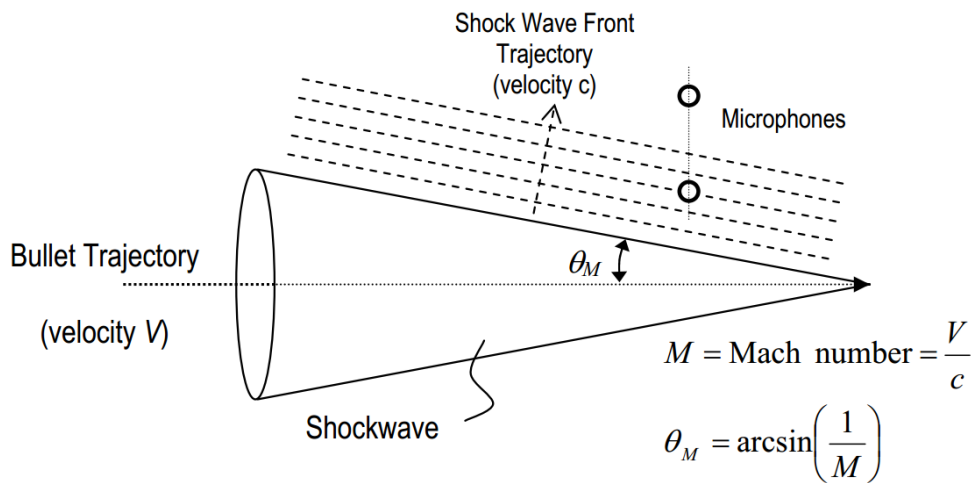


Figure : (2.1) Supersonic bullet shock wave description.

The acoustic shock wave from the bullet has a very rapid rise to a positive overpressure maximum, followed by a corresponding under-pressure minimum. As the shock wave propagates the nonlinear behavior of the air causes the pressure disturbance to form an "N" shape with a rapid onset, a ramp to the minimum pressure, and then an abrupt offset. The time interval, T, of the "N" wave between the maximum over- and under-pressure instants is proportional to the size of the projectile. An expression for the "N" wave time interval is given by:

$$T \approx 1.82 \left(\frac{d}{c} \right) \left(\frac{Mx}{l} \right)^{\frac{1}{4}}$$

Where d is the bullet diameter, l is the bullet length, c is the speed of sound, M is the Mach Number, and x is the distance between the bullet's trajectory and the microphone at the point of closest approach (perpendicular distance between the bullet's path and the microphone). A typical bullet a few centimeters long has an inter shock interval of less than 200 μsec , as shown in Figure (2.2).

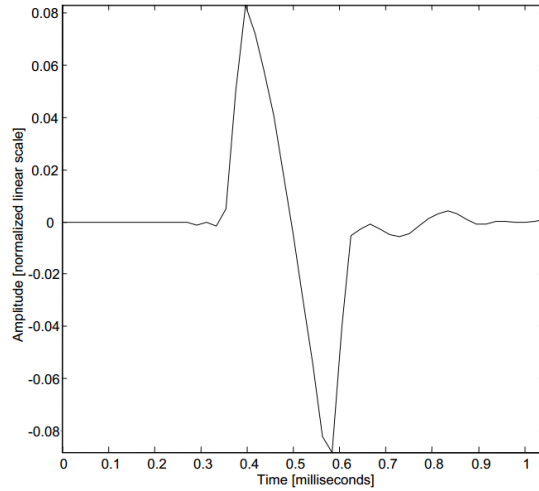


Figure : (2.2) Shock wave recording (“N” wave)

If solid surfaces are present nearby, the passing shock Wave cone will be partially absorbed and partially reflected by the surface. Thus, a microphone in the vicinity will pick up both the original shock wave and the reflected shock wave with a delay corresponding to the path length difference. The ground reflection is depicted in Figure (2.3).

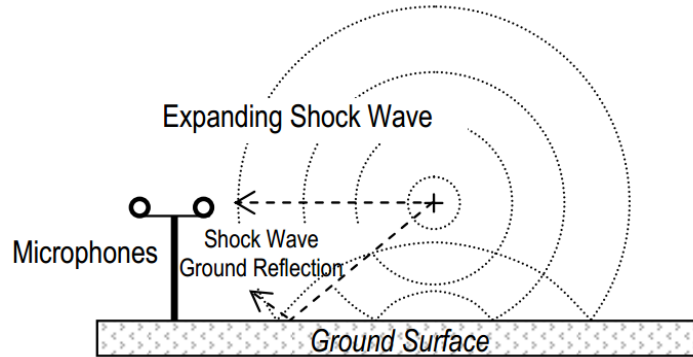


Figure : (2.3) Shock wave ground reflection
(elevation view, no scale, bullet into page)

If a supersonic projectile's journey from the firearm to the target is more than a few tens of meters, the effects of drag-induced deceleration may need to be taken into account. The bullet is slowed by friction with the air and due to the conversion of its kinetic energy in to the acoustic shockwave. As the projectile's speed decreases down range, the shock wave Mach angle (θ_M) increases from its initial value where the bullet leaves the muzzle toward 90° , before the shock wave vanishes as the bullet slows to below the speed of sound. Thus, the actual shock wave boundary is convex rather than straight, as depicted in Figure (2.4).

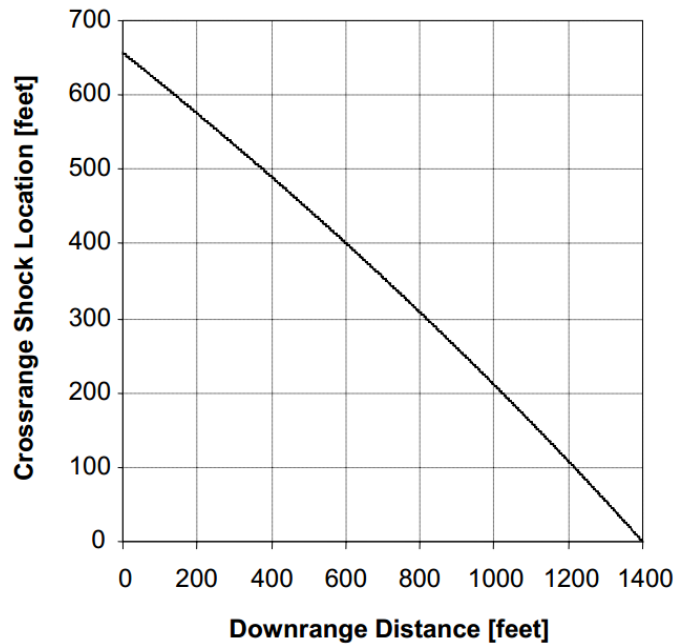


Figure : (2.4) Shock wave front for NATO FNM 83-23 bullet (2750 ft/sec at muzzle, 1980 ft/sec at 1400 feet down range).

2.4. Mechanical action:

For some firearms the sound of the mechanical action may be detectable. This includes the sound of the trigger and hammer mechanism, the ejection of spent cartridges, and the positioning of new ammunition by the gun's automatic or manual loading system. The mechanical action is, of course, generally much quieter than the muzzle blast and projectile shock wave, so this acoustical signal is only relevant if the microphone is located close enough to the firearm to pick up these subtle, telltale sounds. For example, personal surveillance recordings or recorded phone conversations that take place in proximity to the shooter may contain this information.

2.5. Surface vibration:

Acoustic vibration may also be carried through the ground or other solid surfaces. The sound of gunshots, ordnance explosions, and similar impulsive sounds can cause detectable vibratory signals propagating through the ground many tens of meters from the source. Sound propagation in rock and soil is typically at least 5 times faster than the speed of sound in air, so calculations to correlate surface vibratory motion and the subsequent airborne sound arrival may be productive. In summary, the primary acoustical evidence available from a gunshot can include the muzzle blast, the projectile shock wave for supersonic bullets, and possibly the sound of the firearm's mechanical action and ground vibration, if the microphone is sufficiently close to the gun.

2.6. Example Gunshot Characteristics:

Figure (2.5) shows the recorded acoustic data for a Winchester 308 rifle fired horizontally toward the microphones at a distance of approximately 9 meters. The bullet speed (V) for the particular ammunition used was 2728 ft/sec (831.5 m/sec) and the speed of sound (c) was 1075 ft/sec (328 m/sec) at approximately 20°F (-7°C). The resulting Mach Number (V/c) was $M = 2.54$, giving a Mach Angle (θ_M) of 23.2°.

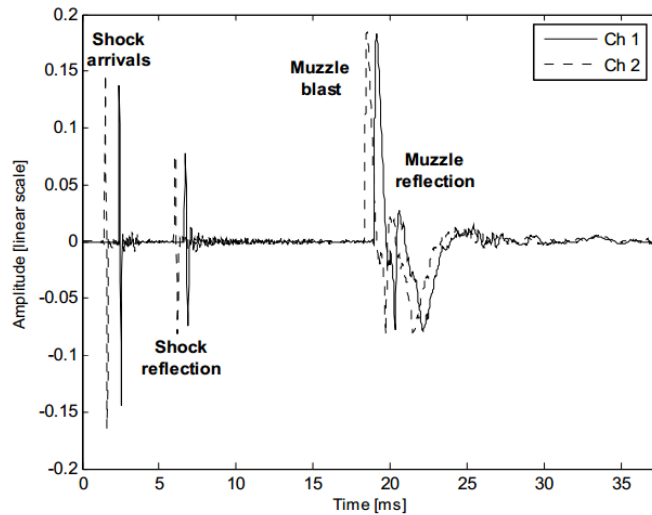


Figure : (2.5) Two-channel gunshot recording, $M=2.54$, oblique trajectory toward the microphones

The arrival of the supersonic bullet's shock wave at the microphones is visible in Figure (2.5), first at microphone 2 and then at microphone 1, with the time delay between channels corresponding to the time required for the shock wave to propagate at the speed of sound from the first microphone to the second. The shock wave cone expanding behind the bullet reaches the microphones relatively quickly when the bullet trajectory is toward the microphones because the projectile is moving at more than 2.5 times the speed of sound. The next significant event is the arrival of the shock wave reflection from the ground. Note that the reflection is of slightly lower amplitude due to the ground absorption and the longer propagation path taken by the reflected energy. Next, the acoustic signature of the muzzle blast arrives at the microphones after having propagated at the speed of sound from the firearm position to the microphones. Finally, the muzzle blast reflection from the ground arrives at the microphones at a delay corresponding to the down-and-up propagation path of the reflection.

The second example uses the same ammunition but a firing trajectory perpendicular to the line connecting the microphones, passing approximately 8 meters from microphone 2. The resulting acoustic recording is shown in Figure (2.6). In this case the propagation of the bullet's trailing

shock wave is essentially parallel to the path of the muzzle blast, resulting in a more nearly coincident arrival of the bullet shock and the blast signatures.

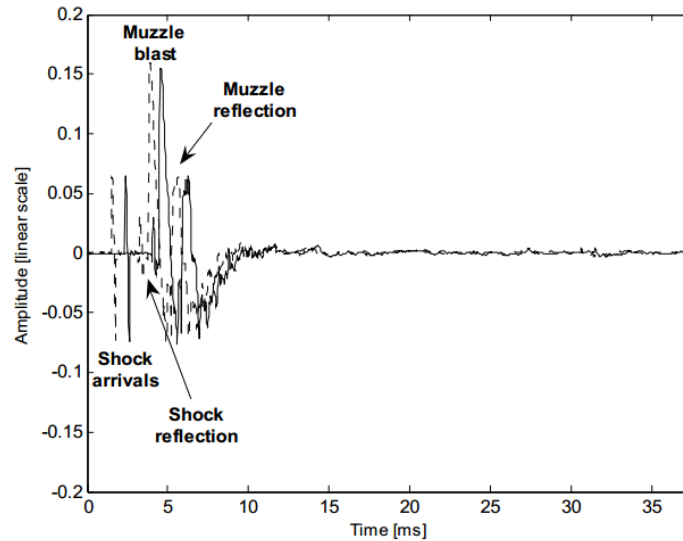


Figure : (2.6) Two-channel gunshot recording, $M=2.54$, perpendicular trajectory, 8 meter offset

The third example again uses the same ammunition and firing trajectory perpendicular to the line connecting the microphones, but unlike the second example the trajectory passes less than 1 meter from microphone 1. The resulting acoustic recording is shown in Figure (2.7). The passage of the bullet very close to the microphones gives a strong initial shock wave arrival. The shock wave reflection arrives nearly simultaneously at the two microphones because the ground reflection paths for this geometry are nearly coincident. Similarly, the muzzle blast arrives nearly simultaneously at the two microphones due to the coincident acoustical paths.

The final example, Figure (2.8), depicts the result when the rifle's muzzle is pointed away from the microphones. In this situation the projectile's expanding shock wave cone does not intercept the microphones. The directionality of the muzzle blast is also evident: the muzzle signature is of lesser amplitude than for the shots made with the muzzle facing the microphones.

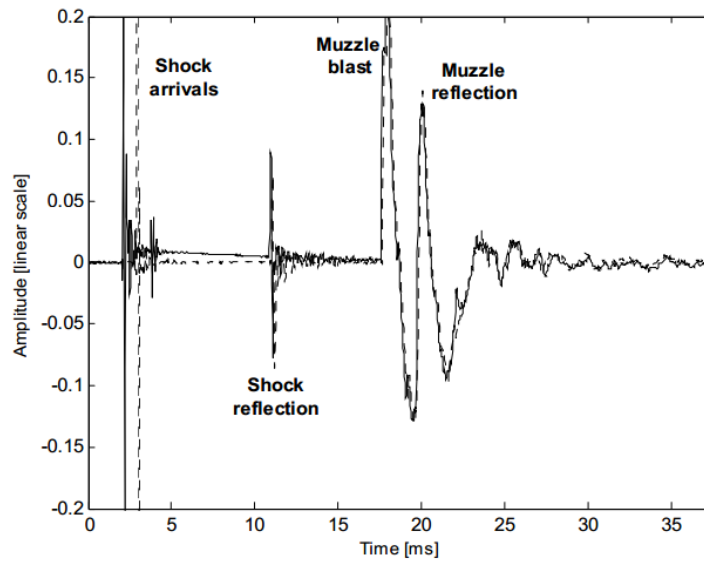


Figure : (2.7) Two-channel gunshot recording
 $M=2.54$, perpendicular trajectory, <1 meter offset

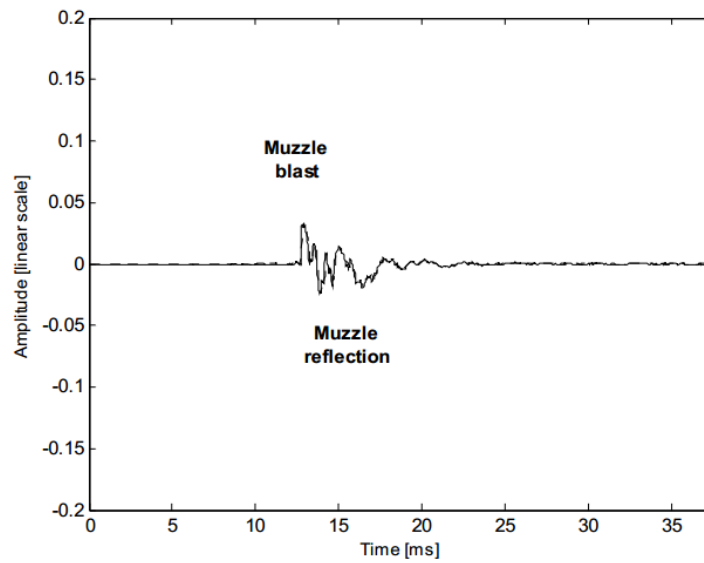


Figure : (2.8) Two-channel gunshot recording, $M=2.54$, opposing trajectory
 (muzzle pointed away from microphones)

Chapter 3

WIRELESS POSITIONING Systems

3.1. Introduction:

Positioning systems determine the location of a person or an object either relative to a known position or within a coordinate system. In the last few decades, various positioning systems have been motivated by demand and have been developed. Some of the applications of positioning systems include (but are not limited to) law enforcement, security, road safety, tracking personnel, vehicles, and other assets, situation awareness, and mobile ad hoc networks.

As shown in Figure (3.1), positioning systems can be classified into two categories:

1. Global Positioning
2. Local Positioning

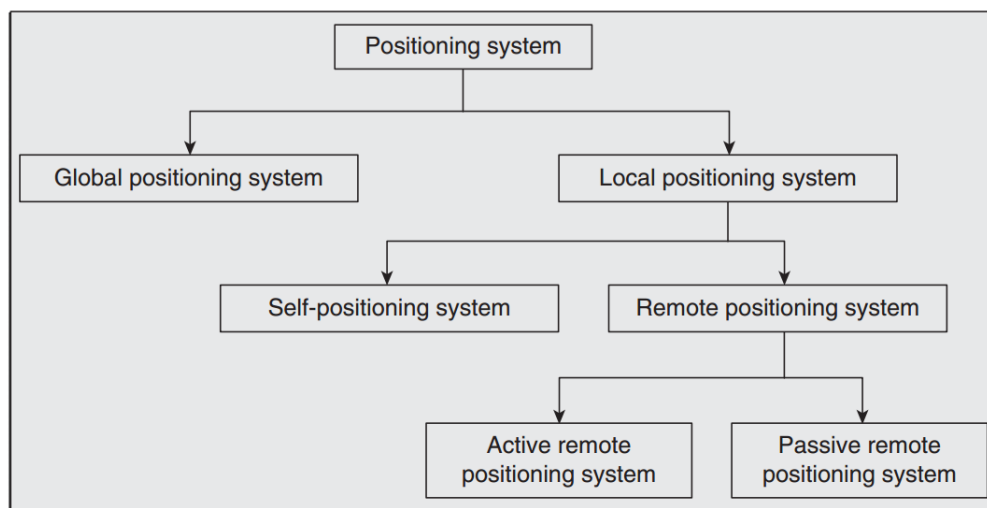


Figure : (3.1) Positioning system classification.

Global positioning systems (GPSs) allow each mobile to find its own position on the globe. A local positioning system (LPS) is a relative positioning system and can be classified into self and remote positioning. Self-positioning systems allow each person or object to find its own position with respect to a static point at any given time and location. An example of these systems is the inertial navigation system (INS).

Remote positioning systems allow each node to find the relative position of other nodes located in its coverage area. Here, nodes can be static or dynamic. Remote positioning systems themselves are divided into:

1. Active target remote positioning.
2. Passive target remote positioning.

In the first case, the target is active and cooperates in the process of positioning, while in the second, the target is passive and noncooperative. Examples of active target positioning systems are radio frequency identification (RFID), wireless local positioning systems (WLPSs), and traffic alert and collision avoidance systems (TCAS). Examples of passive target positioning systems are tracking radars and vision systems.

3.2. Basic methods used in positioning systems:

Here, the fundamental techniques of positioning systems are explained. Different combinations of these techniques form the basis of various positioning systems.

3.2.1. TOA Estimation :

TOA estimation allows the measurement of distance, thus enabling localization. Here, multiple base nodes collaborate to localize a target node via triangulation. It is assumed that the positions of all base nodes are known. If these nodes are dynamic, a positioning technique such as GPS is used to allow base nodes to localize their positions (GPS – TOA positioning).

In some circumstances, multiple base nodes may cooperate to find their own position before any attempt to localize a target node.

Assuming known positions of base nodes and a coplanar scenario, three base nodes and three measurements of distances (TOA) are required to localize a target node (see Figure. 1.2 a). In a non-coplanar case, four base nodes are required. Using the measurement of distance, the position of a target node is localized within a sphere of radius R_i with the receiver i at the center of the sphere where R_i is directly proportional to the TOA τ_i as shown in Figure (1.2 a). The localization of the target node can be carried out either by base nodes using a master station or by the target node itself.

Although TOA seems to be a robust technique, it has a few drawbacks:

1. It requires all nodes (base nodes and target nodes) to precisely synchronize: A small timing error may lead to a large error in the calculation of the distance R_i .
2. The transmitted signal must be labeled with a time stamp in order to allow the base node to determine the time at which the signal was initiated at the target node. This additional time stamp increases the complexity of the transmitted signal and may lead to an additional source of error.
3. The positions of the base nodes should be known; thus, either static nodes or GPS - equipped dynamic nodes should be used.

3.2.2. Time Difference Of Arrival (TDOA) Estimation:

As the name suggests, TDOA estimation requires the measurement of the difference in time between the signals arriving at two base nodes. Similar to TOA estimation, this method assumes that the positions of base nodes are known. The TOA difference at the base nodes can be represented by a hyperbola. A hyperbola is the locus of a point in a plane such that the difference of distances from two fixed points (called the foci) is a constant.

Assuming known positions of base nodes and a coplanar scenario, three base nodes and two TDOA measurements are required to localize a target node (see Figure 3.2 b). As shown in the figure, the base station that first receives the signal from the target node is considered as the reference base station. The TDOA measurements are made with respect to the reference base station. For a noncoplanar case, the positions of four base nodes and three TDOA measurements are required.

TDOA addresses the first drawback of TOA by removing the requirement of synchronizing the target node clock with base node clocks. In TDOA, all base nodes receive the same signal transmitted by the target node. Therefore, as long as base node clocks are synchronized, the error in the arrival time at each base node due to unsynchronized clocks is the same.

As shown in Figure (3.2 c), TOA is the time duration (or the relative time) between the start time (t_s) of the signal at the transmitter (target node) and the end time (t_i) of the transmitted signal at the receiver (base node B_i). However, as shown in Figure (3.2 c), TDOA is the time difference between the end times (t_i and t_j) of the transmitted signal at two receivers (base nodes B_i and B_j). Thus, in the TDOA technique, only base nodes' clocks need to be synchronized to ensure minimum measurement error. In general, the complexity of target node clock synchronization is higher compared with base node clock synchronization. This is mainly due to the use of quartz clocks at target nodes, which are not as precise as atomic clocks that are generally used for timing at base nodes.

The base node clock can be synchronized externally by using a backbone network or internally using timing standards provided at the nodes. The fact that synchronization of target nodes is not required enables many applications for TDOA-based systems. For example, in battlefield applications, a rescue team may localize the position of a soldier using its beacon signal without the need of synchronization of rescue team clocks with that of the soldier .

With respect to the second drawback of TOA, the transmitted signal from the target node in TDOA need not contain a time stamp, since a single TDOA measurement is the difference in the arrival time at the respective base nodes. This simplifies the structure of transmitted signals and removes potential sources of error. This advantage of TDOA is again exploited by many applications such as emergency call localization on highways and sound source localization by an artificially intelligent humanoid robot.

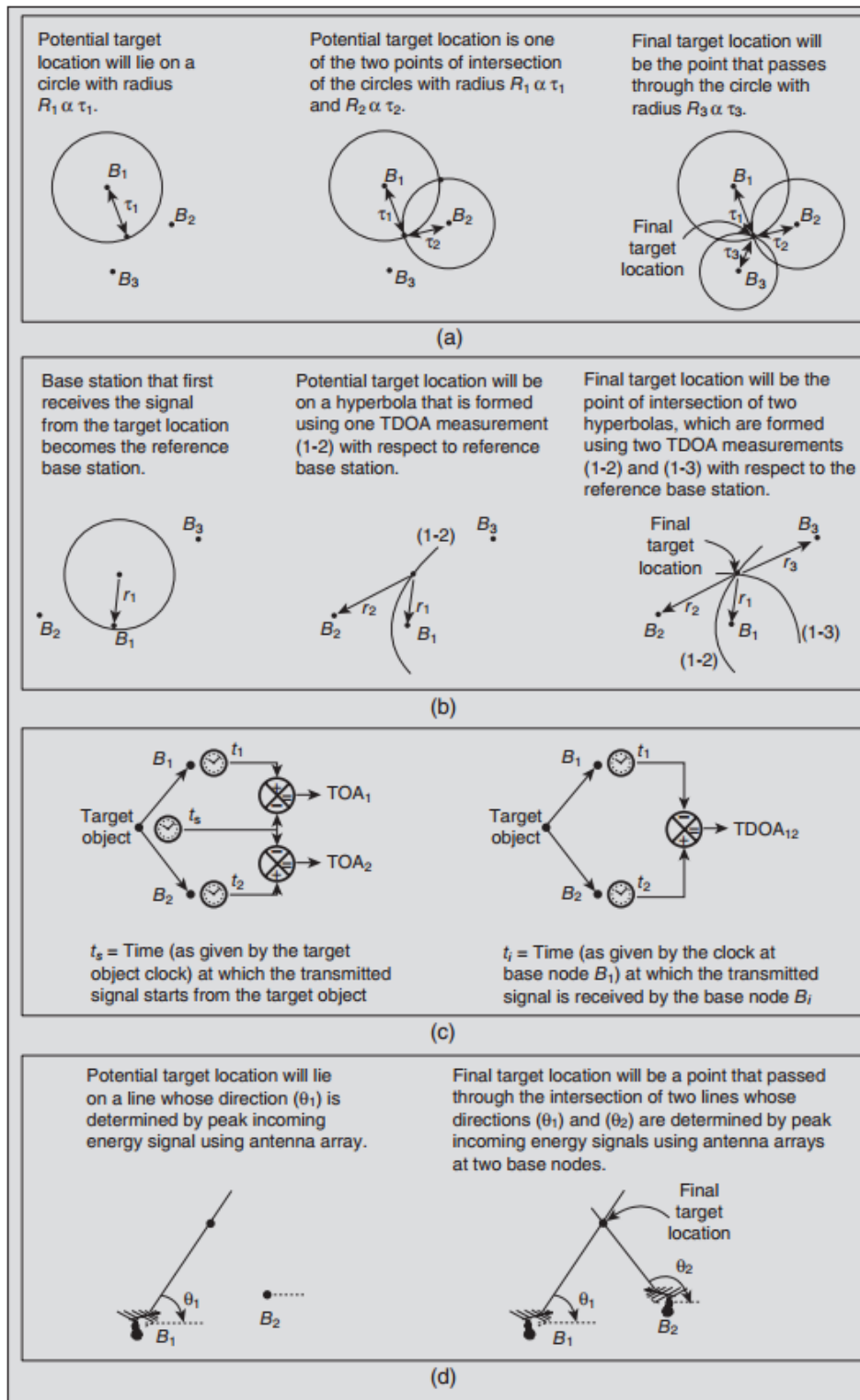


Figure : (3.2) (a) Operation of TOA and RSSI, (b) operation of TDOA, (c) comparison of TOA and TDOA calculations, and (d) operation of DOA

3.2.3. DOA Estimation :

In DOA estimation, base nodes determine the angle of the arriving signal (see Figure 3.2 d). To allow base stations to estimate DOA, they should be equipped with antenna arrays, and each antenna array should be equipped with radio frequency (RF) front-end components. However, this incurs higher cost, complexity, and power consumption. Similar to TOA and TDOA estimation, in DOA estimation, the positions of base nodes should be known. However, unlike TOA and TDOA, for the known position of a base node and a coplanar scenario, only two base nodes along with two DOA measurements are required. For a non-coplanar case, three base nodes are required. To determine the DOA, the main lobe of an antenna array is steered in the direction of the peak incoming energy of the arriving signal.

3.2.4. RSSI :

Similar to the TOA, in RSSI, multiple base nodes collaborate to localize a target node via triangulation (see Figure 3.2 a). However, instead of measuring the TOA at base nodes, the estimation is carried out using the received signal strength (RSS). In this method, the strength of the received signal indicates the distance traveled by the signal. Assuming that the transmission strength and channel (or environment in which the signal is traveling) characteristics are known, for a coplanar case, three base nodes and three RSS measurements are required.

A comparison summary for the four measurement models is provided in Table (1.1) .

Model	Location Information	Advantages	Disadvantages
TOA	Range	Accuracy is high.	Time synchronization across source and all receivers is needed. LOS is assumed.
TDOA	Range difference	Accuracy is high. Time synchronization at source is not required.	LOS is assumed.
RSS	Range	Simple and inexpensive Time synchronization is not required.	Accuracy is low.
DOA	Bearing	Only at least two receivers are needed. Time synchronization is not required.	Smart antennas are needed. LOS is assumed.

Table : (1.1) Comparison of Different Measurement Models

3.3. Acoustic source localization:

The process of determining the location of an acoustic source relative to some reference frame is known as acoustic source localization. Acoustic source present in the near-field can be localized with knowledge of the time difference of arrivals (TDOAs) measured with pairs of microphones. The speed of sound in the medium in which the acoustic source is present is known. With continued investigation over the last two decades, the time delay estimation (TDE) based localization has become the technique of choice. The location of a target is found using a two-dimensional-three-element microphone array at least. A pair of microphones gives the DOA only. Since the target has two degrees of freedom, the DOA estimated would give only the direction of the source.

Chapter 4

Position Location Estimation

4.1. Direction of Arrival Estimation:

The existing strategies of source localization are of two types. One is Time Delay Estimation (TDE) based (also called as indirect methods) and the other is direct methods where the source location is computed in one stage. We have implemented the TDE based method, since they are easily realizable in real-time, unlike the direct methods which are computationally intensive.

4.2. Time Difference Of Arrival (TDOA):

Let m_i for $i \in [1, M]$ be the three dimensional vectors representing the spatial coordinates of the i_{th} microphone and 's' as the spatial coordinates of sound source. We excite the source 's' and measure the time difference of arrivals. Letting 'c' as the speed of sound in the acoustical medium (air) and $\| \cdot \|$ is the Euclidean norm. The TDOA for a given pair of microphones and the source is defined as the time difference between the signals received by the two microphones. Let $TDOA_{ij}$ be the TDOA between the i_{th} and j_{th} microphone when the source 's' is excited. It is given by

$$TDOA_{ij} = \frac{(\|m_i - s\| - \|m_j - s\|)}{c}$$

TDOA's are then converted to time delay estimations (TDE's) and path differences. This is depicted in Figure (4.1)

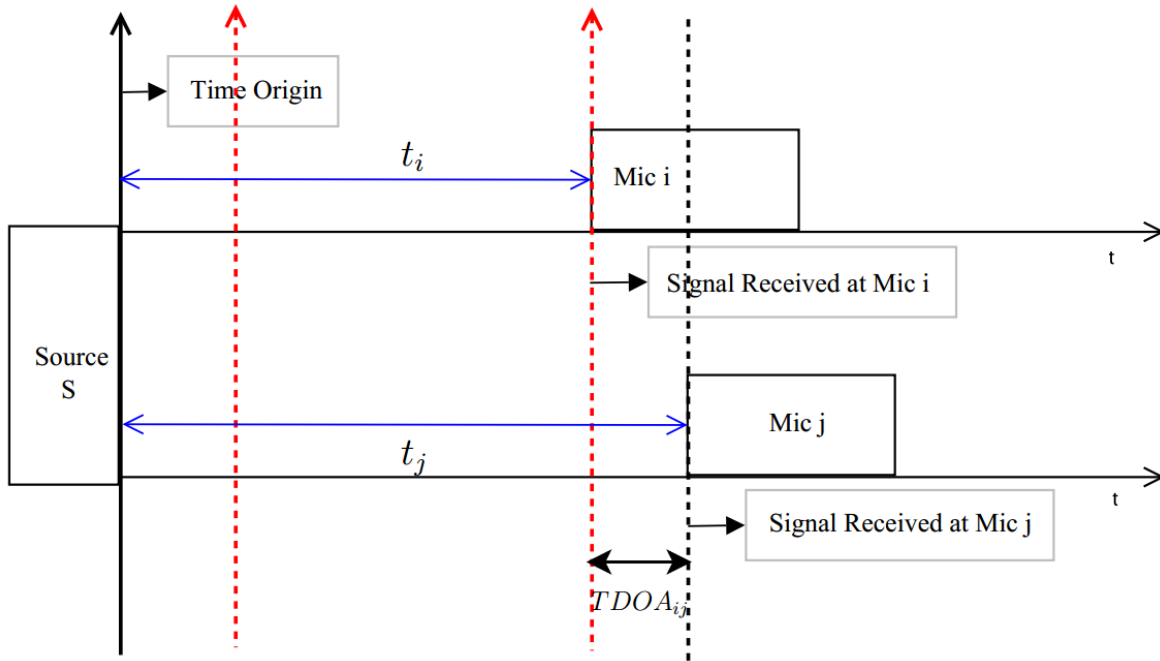


Figure : (4.1) Schematic depicting the signal receiving time and TDOA.

4.3. Restrictions on the microphones array geometry:

In this section we derive a relationship between the frequency content of the incident signal and the maximum allowed separation between each pair of microphones in the array. The maximum phase difference is restricted to $|\pi|$. Any phase difference out of the range of $-\pi$ and π is wrapped around to within this range. This places an important restriction on the array geometry when performing DOA estimation.

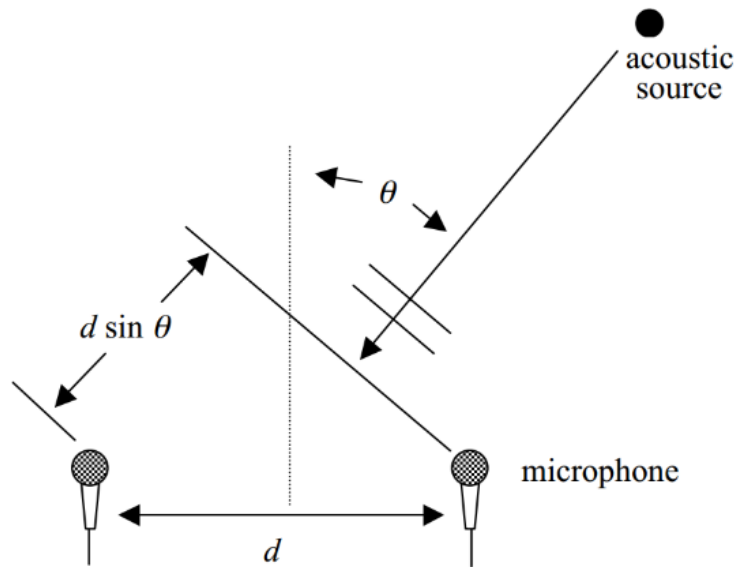


Figure : (4.2) Two-element microphone array.

Consider a signal incident on the pair of microphone as shown in Figure (4.2) at an angle θ . Let the broad band signal have a maximum frequency of f_{\max} . At f_{\max} , if we restrict the phase difference between signals of pair of microphones to be less than or equal to π , then we require

$$2\pi f_{\max} \tau \leq \pi$$

And

$$\tau = \frac{d \sin \theta}{\nu}$$

Where

τ = signal time delay between the two microphones.

d = distance between the pair of microphones.

θ = incident angle.

ν = velocity of sound.

Rearranging these terms, we have

$$d \leq \frac{1}{2} \left(\frac{\nu}{f_{\max}} \right) \frac{1}{\sin \theta}$$

For $\sin \theta|_{\max} = 1$ and since ν/f_{\max} is same as λ_{\min} , the minimum wave length present in the signal.

$$\Rightarrow d \leq \frac{\lambda_{min}}{2} = \frac{v}{2f_{max}}$$

This means that the distance between any pair of microphones in the array should not exceed half the minimum wavelength present in the signal. This condition becomes very important when we perform TDE from phase difference estimates of the signals.

4.4. Conventional DOA methods:

There are various techniques that can be used to compute pair-wise time delays, such as the generalized cross correlation (GCC) method. The phase transform (PHAT) is the most commonly used pre-filter for the GCC. Computation of the time delay between signals from any pair of microphones can be performed by first computing the cross-correlation function of the two signals. The lag at which the cross-correlation function has its maximum is taken as the time delay between the two signals.

4.4.1. Cross-correlation:

Cross-correlation of two signals is the convolution of one with the complex conjugate of the other. The cross-correlation $R_{x_1, x_2}(t)$ of two signals x_1 and x_2 is:

$$R_{x_1, x_2}(t) = x_1 \star x_2 \equiv x_1(-t) \otimes x_2(t)$$

Where \star denotes cross-correlation; \otimes denotes convolution defined by

$$x_1(t) \otimes x_2(t) = \int_{-\infty}^{\infty} x_1(\tau) x_2(t - \tau) d\tau$$

Cross-correlation determines how correlated two signals are. Two signals that are identical but time-shifted by a certain time-delay will have a cross-correlation function with a strong maximum peak at that time-delay point (Stein, 1981). However, when reverberation distorts the input signals, each reverberation causes an extra peak in the cross-correlation function as side lobes. When the input signal is very periodic the cross-correlation function is also very periodic in form. Each of the periodic peaks would have its own side lobes which sum with the existing peaks. This makes it difficult to determine which peak is the central time-delay peak and which are just reverberation side lobes. Background noise that exists in the signals also affects the plots in two ways depending on whether the noise is random or whether there is a localized noise source. Spatially random noise would create random errors in the plots whereas localized noise would produce extra correlation peaks relative to the time delay of the noise source location. Spatially random noise may arise from a large number of distributed noise sources such as computers; a large number of reflections will also tend to de-correlate the noise sources.

4.4.2. Generalized Cross-correlation :

The generalized cross-correlation can be explained using the following equations. The original cross-correlation $R_{x_1, x_2}(t)$ is related to the cross power spectral density function $G_{x_1, x_2}(f)$ by the Fourier transform relationship

$$R_{x_1, x_2}(t) = \int_{-\infty}^{\infty} G_{x_1, x_2}(f) e^{j2\pi ft} df$$

The generalized cross-correlation has an additional weighting value $\psi(f)$ in the frequency domain, before the integration/summation step and is of the form

$$Rg_{x_1, x_2}(t) = \int_{-\infty}^{\infty} \psi(f) G_{x_1, x_2}(f) e^{j2\pi ft} df$$

The weighting value is chosen from a number of different proposed methods, each with their advantages and disadvantages. The ordinary cross-correlation method would have $\psi(f) = 1$, while The GCC-PHAT uses a weighting of

$$\psi(f) = \frac{1}{|G_{x_1, x_2}(f)|}$$

which produces

$$Rg_{x_1, x_2}(t) = \int_{-\infty}^{\infty} \frac{G_{x_1, x_2}(f)}{|G_{x_1, x_2}(f)|} e^{j2\pi ft} df$$

Essentially the GCC-PHAT normalizes the resulting cross spectral power density of the two signals to a constant value which effectively pre-whitens the cross-correlation function. This pre-whitening equalizes the amplitude of the signals across the frequency band leaving only the phase information. This helps to reduce the effects of reverberation on the accuracy of the TDOA estimates.

4.4.3. Eigenvalue Decomposition (ED) Method :

The ED method is based on estimating the impulse response between the two signals. A model of the signals received $x_i(n)$, $i= 1, 2$, can be expressed as

$$x_i(n) = g_i \otimes s(n) + b_i(n)$$

Where $s_i(n)$ is the source, g_i is the discrete time impulse response of the channel between the source and receiver and $b_i(n)$ is additive noise.

Simplifying previous equation by removing additive noise, we have

$$x_1(n) = g_1 \otimes s(n), \quad x_2(n) = g_2 \otimes s(n)$$

Therefore assuming that the system (room) is linear, time invariant and noise free

$$x_1(n) \otimes g_2 = g_1 \otimes s(n) \otimes g_2 = g_1 \otimes g_2 \otimes s(n) = g_1 \otimes x_2(n).$$

From this we have the relation

$$\underline{x}_1^T(n) \mathbf{g}_2 = \underline{x}_2^T(n) \mathbf{g}_1$$

where \mathbf{x}_i and \mathbf{g}_i are vectors of the signals received and corresponding impulse responses respectively, where

$$\underline{x}_i(n) = \begin{bmatrix} x_i(n) \\ x_i(n-1) \\ \vdots \\ x_i(n-N+1) \end{bmatrix}$$

are the samples along the N tap filter used to model the impulse response.

The covariance matrix of the two signals is

$$\mathbf{R} = \begin{bmatrix} \mathbf{R}_{x_1 x_1} & \mathbf{R}_{x_1 x_2} \\ \mathbf{R}_{x_2 x_1} & \mathbf{R}_{x_2 x_2} \end{bmatrix}$$

where

$$\mathbf{R}_{x_i x_j} = E\{\mathbf{x}_i(n) \mathbf{x}_j^T(n)\}, i, j = 1, 2.$$

Let

$$\mathbf{u} = \begin{bmatrix} \mathbf{g}_2 \\ -\mathbf{g}_1 \end{bmatrix}.$$

We have then

$$\begin{aligned} \mathbf{R}\mathbf{u} &= \begin{bmatrix} \mathbf{R}_{x_1 x_1} \mathbf{g}_2 - \mathbf{R}_{x_1 x_2} \mathbf{g}_1 \\ \mathbf{R}_{x_2 x_1} \mathbf{g}_2 - \mathbf{R}_{x_2 x_2} \mathbf{g}_1 \end{bmatrix} \\ &= \begin{bmatrix} E\{\mathbf{x}_1 \mathbf{x}_1^T\} \mathbf{g}_2 - E\{\mathbf{x}_1 \mathbf{x}_2^T\} \mathbf{g}_1 \\ E\{\mathbf{x}_2 \mathbf{x}_1^T\} \mathbf{g}_2 - E\{\mathbf{x}_2 \mathbf{x}_2^T\} \mathbf{g}_1 \end{bmatrix} \\ &= \begin{bmatrix} E\{\mathbf{x}_1 \mathbf{x}_1^T \mathbf{g}_2\} - E\{\mathbf{x}_1 \mathbf{x}_2^T \mathbf{g}_1\} \\ E\{\mathbf{x}_2 \mathbf{x}_1^T \mathbf{g}_2\} - E\{\mathbf{x}_2 \mathbf{x}_2^T \mathbf{g}_1\} \end{bmatrix} \\ &= \begin{bmatrix} 0 \\ 0 \end{bmatrix} = 0 \end{aligned}$$

meaning that vector \mathbf{u} is the eigenvector of \mathbf{R} corresponding to an eigenvalue of 0.

\mathbf{u} is the estimated impulse response from the source to a microphone. It is calculated using

a Least Mean Square (LMS) algorithm with the following equations:

$$e(n) = \mathbf{u}^T(n)\mathbf{x}(n)$$

$$\mathbf{u}(n+1) = \frac{\mathbf{u}(n) - \mu e(n)\mathbf{x}(n)}{\|\mathbf{u}(n) - \mu e(n)\mathbf{x}(n)\|}$$

where $e(n)$ is the error signal and μ is the step size.

The aim is not to accurately estimate the impulse responses g_1 and g_2 but to find the time-delay. It is sufficient to just detect the two direct paths. By initializing a tap equal to 1 in the middle of the first half of \mathbf{u} (i.e. in the middle of g_2) and having everything else zero that particular peak will always be dominant. A “mirror” effect will appear in the second half of \mathbf{u} (i.e. in g_1) in the form of a negative peak that will dominate. The relative position of this peak compared with the original peak in the first half of \mathbf{u} is the time-delay.

4.5. Hyperbolic position location :

Hyperbolic position location (PL) estimation is accomplished in two stages. The first stage involves estimation of the time difference of arrival (TDOA) between the microphones through the use of time-delay estimation techniques. The estimated TDOAs are then utilized to make range difference measurements. This would result in a set of nonlinear hyperbolic range difference equations. The second stage is to implement an efficient algorithm to produce an unambiguous solution to these nonlinear hyperbolic equations. The solution produced by these algorithms result in the estimated position location of the source. The following sections discuss the techniques used to perform hyperbolic position location of the sound source.

Accurate position location (PL) estimation of a source requires an efficient hyperbolic position location estimation algorithm. Once the TDOA information has been measured, the hyperbolic position location algorithm will be responsible for producing an accurate and unambiguous solution to the position location problem. Algorithms with different complexity and restrictions have been proposed for position location estimation based on TDOA estimates. When the microphones are arranged in non-collinear fashion, the position location of a sound source is determined from the intersection of hyperbolic curves produced from the TDOA estimates. The set of equations that describe these hyperbolic curves are non-linear and are not easily solvable. If the number of nonlinear hyperbolic equations equals the number of unknown coordinates of the source, then the system is consistent and a unique solution can be determined from iterative techniques. For an inconsistent system, the problem of solving for the position location of the sound source becomes more difficult due to non-existence of a unique solution.

4.5.1. Localization Algorithm :

The Ho-Chan method (1994) is the TDOA localization method investigated in this project. The basis behind this method relies on minimizing a least squares (LS) estimator. The method utilizes the next relationship in between the source coordinates (x, y) and distance r_i when finding the coordinate estimates:

$$(x_i - x)^2 + (y_i - y)^2 = r_i^2$$

Where (x_i, y_i) are the coordinates of sensor i.

The method initially assumes that the three variables x, y and r_i are independent and uses LS to find an initial estimate.

Without any loss of generalization, let microphone 1 to be the reference sensor. Thus for $i= 1$ the localization equation becomes

$$(x_1 - x)^2 + (y_1 - y)^2 = r_1^2.$$

$$\text{Let } X = \begin{bmatrix} (x_2 - x_1) & (y_2 - y_1) \\ (x_3 - x_1) & (y_3 - y_1) \\ \vdots & \vdots \\ (x_N - x_1) & (y_N - y_1) \end{bmatrix}, \quad K_i = x_i^2 + y_i^2 \text{ for } i = 1 \text{ to } N$$

Where N is the number of sensors.

With $i = 2 : N$, subtracting previous equation gives a set of equations which can be written in the form

$$\begin{bmatrix} x \\ y \end{bmatrix} = C r_1 + D$$

Where

$$C = (X^T X)^{-1} X^T \begin{bmatrix} -r_{2,1} \\ -r_{3,1} \\ \vdots \\ -r_{N,1} \end{bmatrix}, \quad D = (X^T X)^{-1} X^T \left(\frac{1}{2} \right) \begin{bmatrix} -r_{2,1}^2 + K_2 - K_1 \\ -r_{3,1}^2 + K_3 - K_1 \\ \vdots \\ -r_{N,1}^2 + K_N - K_1 \end{bmatrix}.$$

Where $r_{i,j}$, is the TDOA distance between microphones j and i.

By assuming that the variables x , y and r_1 are independent, the error vector ψ is defined as

$$\mathbf{h} - \mathbf{G}_a \mathbf{z}_a^0 = \psi$$

Where

$$\mathbf{h} = -\frac{1}{2} \mathbf{B} = \frac{1}{2} \begin{bmatrix} r_{2,1}^2 - K_2 + K_1 \\ r_{3,1}^2 - K_3 + K_1 \\ \vdots \\ r_{N,1}^2 - K_N + K_1 \end{bmatrix}, \quad \mathbf{G}_a = -[\mathbf{X} \quad \mathbf{A}] = -\begin{bmatrix} x_{2,1} & y_{2,1} & r_{2,1} \\ x_{3,1} & y_{3,1} & r_{3,1} \\ \vdots & \vdots & \vdots \\ x_{N,1} & y_{N,1} & r_{N,1} \end{bmatrix},$$

$$\mathbf{z}_a^0 = \begin{bmatrix} x^0 \\ y^0 \\ r_1^0 \end{bmatrix}, \quad \psi = \begin{bmatrix} \psi_2 \\ \psi_3 \\ \vdots \\ \psi_N \end{bmatrix}.$$

\mathbf{z}_a^0 are the true values of

$$\mathbf{z}_a = \begin{bmatrix} x \\ y \\ r_1 \end{bmatrix}$$

Which correspond to the estimated source location (x, y) and the estimated distance between the source and the reference microphone r_1 .

When the true TDOA distances are available $\psi = 0$. In practice this is not the case. The Ho-Chan method involves a Least Square (LS) calculation to minimize ψ :

$$\mathbf{z}_a = (\mathbf{G}_a^T \mathbf{\Psi}^{-1} \mathbf{G}_a)^{-1} \mathbf{G}_a^T \mathbf{\Psi}^{-1} \mathbf{h}.$$

$\mathbf{\Psi}$ is the covariance matrix of ψ and is given by

$$\mathbf{\Psi} = \mathbf{B} \mathbf{Q} \mathbf{B}$$

where

$$\mathbf{B} = \begin{bmatrix} r_2^0 & 0 & \dots & 0 \\ 0 & r_3^0 & & \vdots \\ \vdots & & \ddots & 0 \\ 0 & \dots & 0 & r_N^0 \end{bmatrix}, \quad \mathbf{Q} \text{ is the covariance matrix of the TDOA distances.}$$

In practice Ψ is not known since \mathbf{B} contains the true TDOA distances. The Ho-Chan method approximates \mathbf{z}_a as

$$\mathbf{z}_a \approx (\mathbf{G}_a^T \mathbf{Q}^{-1} \mathbf{G}_a)^{-1} \mathbf{G}_a^T \mathbf{Q}^{-1} \mathbf{h}.$$

\mathbf{B} is estimated from the initial estimates of \mathbf{z}_a from (8) it can be iterated multiple times to produce an even better estimate, but simulations done by Chan and Ho (1994) show that one iteration is sufficient to produce accurate results.

The covariance of \mathbf{z}_a is given by

$$\text{cov}(\mathbf{z}_a) = (\mathbf{G}_a^{0T} \Psi^{-1} \mathbf{G}_a^0)^{-1}$$

where \mathbf{G}_a^0 is identical to \mathbf{G}_a except that it uses the exact values of $r_{2,1} \dots r_{N,1}$ rather than the estimated ones.

Let the elements of \mathbf{z}_a be expressed as

$$\mathbf{z}_a = \begin{bmatrix} z_{a,1} \\ z_{a,2} \\ z_{a,3} \end{bmatrix} = \begin{bmatrix} x^0 + e_1 \\ y^0 + e_2 \\ r_1^0 + e_3 \end{bmatrix}$$

where e_1 , e_2 and e_3 are estimation errors of \mathbf{z}_a .

Chan and Ho define another set of equations:

$$\mathbf{h}' - \mathbf{G}_a' \mathbf{z}_a'^0 = \psi'$$

where

$$\mathbf{h}' = \begin{bmatrix} (z_{a,1} + x_1)^2 \\ (z_{a,2} + y_1)^2 \\ z_{a,3}^2 \end{bmatrix}, \mathbf{G}_a' = \begin{bmatrix} 1 & 0 \\ 0 & 1 \\ 1 & 1 \end{bmatrix}, \quad \mathbf{z}_a' = \begin{bmatrix} (x - x_1)^2 \\ (y - y_1)^2 \end{bmatrix}, \quad \boldsymbol{\psi}' = \begin{bmatrix} \psi_1' \\ \psi_2' \\ \psi_3' \end{bmatrix}.$$

$\boldsymbol{\psi}'$ is the vector of inaccuracies in \mathbf{z}_a . The covariance matrix $\boldsymbol{\Psi}'$ of $\boldsymbol{\psi}'$ is

$$\boldsymbol{\Psi}' = \mathbf{E}[\boldsymbol{\psi}'\boldsymbol{\psi}'^T] = 4\mathbf{B}'\text{cov}(\mathbf{z}_a)\mathbf{B}'$$

where

$$\mathbf{B}' = \begin{bmatrix} (x^0 - x_1) & 0 & 0 \\ 0 & (y^0 - y_1) & 0 \\ 0 & 0 & r_1^0 \end{bmatrix}.$$

\mathbf{B}' can be approximated by using the values in \mathbf{z}_a . A second LS calculation is used to find \mathbf{z}_a'

$$\mathbf{z}_a' = (\mathbf{G}_a'^T \boldsymbol{\Psi}'^{-1} \mathbf{G}_a')^{-1} \mathbf{G}_a'^T \boldsymbol{\Psi}'^{-1} \mathbf{h}'$$

\mathbf{z}_a' is an estimate of $(x - x_1)^2$ and $(y - y_1)^2$ and so a simple conversion will produce x and y estimates:

$$\mathbf{z}_p = \pm \sqrt{\mathbf{z}_a'} + \begin{bmatrix} x_1 \\ y_1 \end{bmatrix}.$$

Since there are two possible solutions for a square root, the correct solution is the one that lies in the region of interest. This can be easily determined by looking at the sign of the initial \mathbf{z}_a estimates. If one of the coordinates is close to zero the square root may become imaginary. In this case the imaginary component should be set to zero (Chan and Ho 1994).

Chapter 5

Practical Result

5.1. Introduction :

This chapter introduces a simulation to a gun finder locator using Matlab. And a circuit to find the direction of gun sound. The circuit is based on atmega8 microcontroller.

5.2. GUI Interface :

The simulation GUI interface is shown in Figure (5.1), the GUI consists of

1) Microphones Parameters:

- Number Of Mics: determines the number of Microphones (Receivers).
- Mic: to choose the number of microphone to set its location.
- X Position: the x position of the microphone with number determined in Mic.
- Y Position: the y position of the microphone with number determined in Mic.

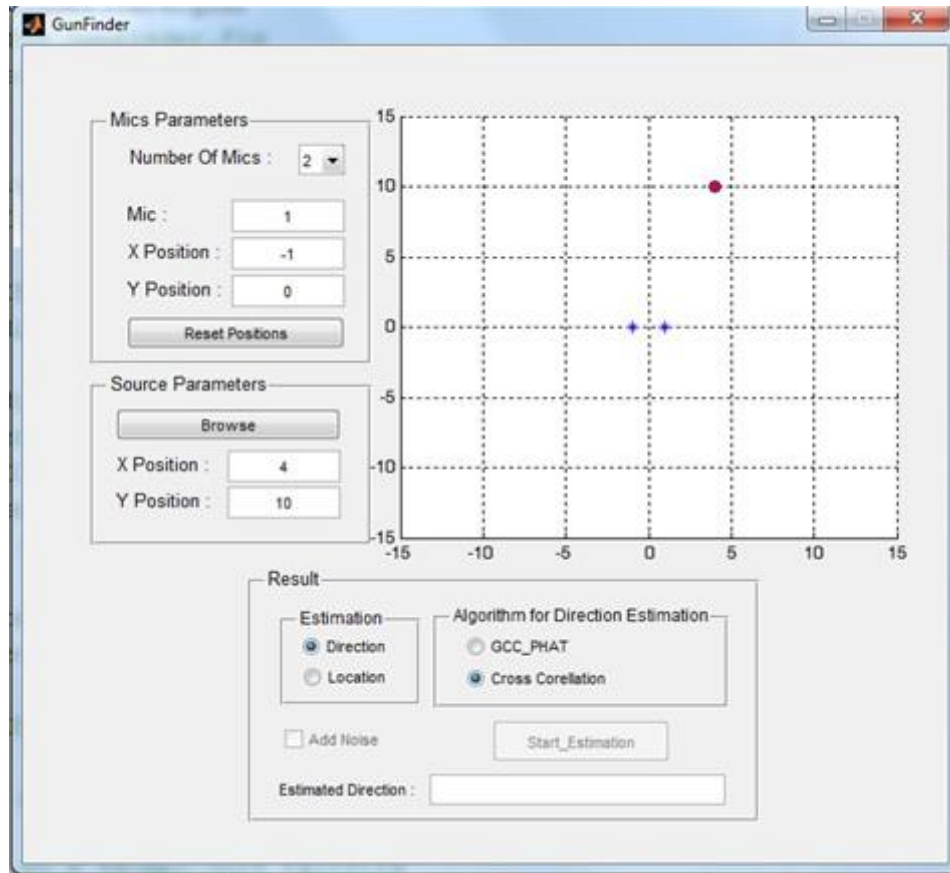


Figure : (5.1) Gun finder GUI interface simulator.

- Reset Positions: to reset (x, y) position of microphones to initial values.
- 2) Source Parameters:
- Browse: to choose wav file with a Gun Sound.
 - X Position: the x position of the Gun.
 - Y Position: the x position of the Gun.
- 3) Result:
- Estimation: to determine localization method, (x, y) location or direction of arrival.
 - Algorithm for direction Estimation: choose algorithm, GCC_Phlat, cross correlation.
 - Add Noise: to add uncertainty in microphones for location estimation method.

- Start Estimation: to start localization estimation process.
- Estimated direction: shows the angle of gun sound arrival for method **Direction**, shows the (x, y) location of the gun for method **Location**.

4) Graph to show the real positions of the microphones and the gun.

5.3. Simulation Result:

5.3.1. Direction of arrival:

First case to simulate is the direction of arrival of gun sound, to find the direction we need at most two microphones, we set microphones in locations

- Mic 1 : (-1,0)
- Mic 2 : (1,0)

And the acoustic source (Gun) in location (4, 10), we use the cross correlation method. Figure (5.2) shows the gun muzzle blast, Figure (5.3) shows the cross correlation between microphones received signal, and the result of simulation is shown in figure (5.4).

If we reset the simulation for another positions of source and microphones with the GCC_phat methods, we get the same result. Figures : (5.5) to (5.8) show the result.

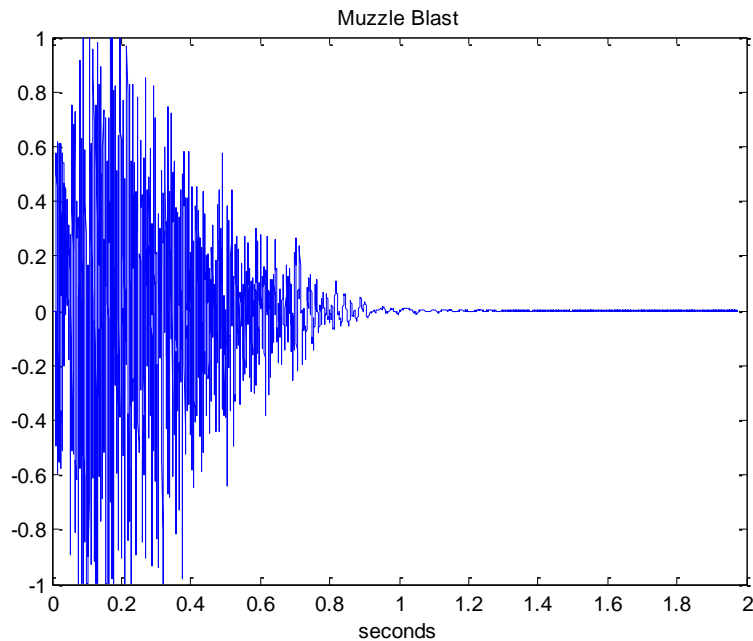


Figure : (5.2) The muzzle blast of gun sound used in simulation.

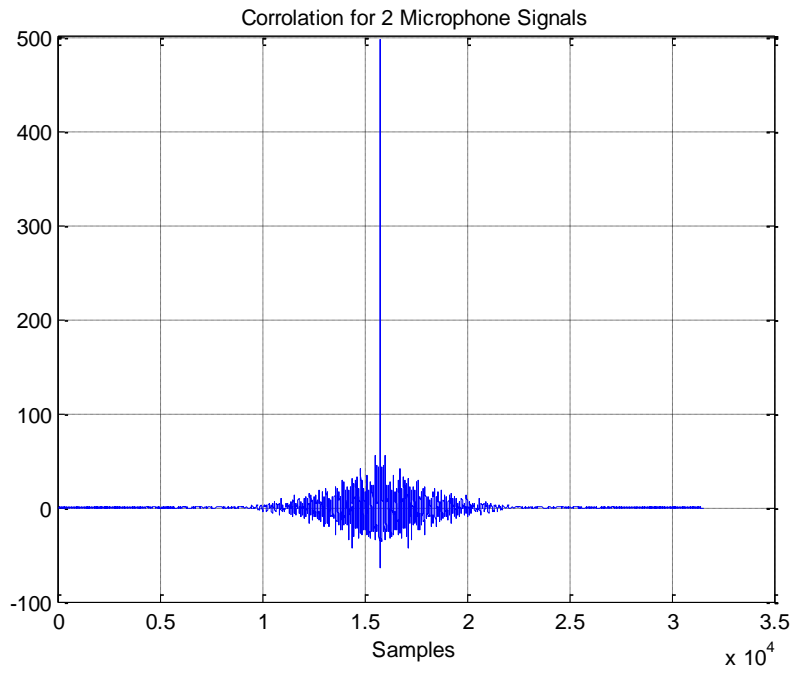


Figure : (5.3) Cross Correlation between microphones signals.

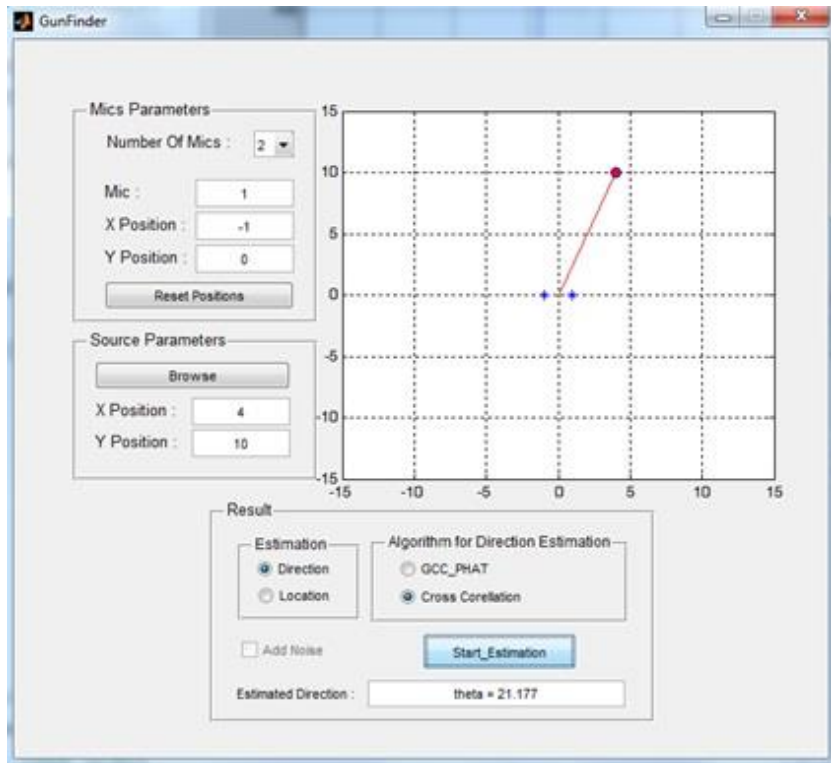


Figure : (5.4) First case simulation result.

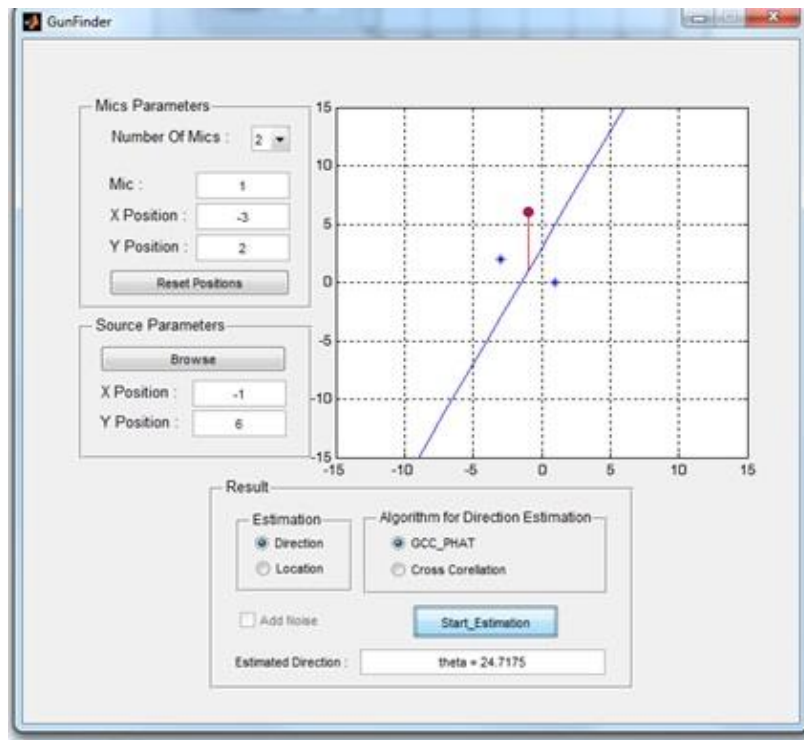


Figure : (5.5) DOA for Target in (-1, 6)
Mics in (-3, 2), (1, 0), GCC_Phats Estimation.

5.3.2. Hyperbolic position location :

Second case is to simulate the hyperbolic position location of gun sound. to find the position we need more receivers than DOA estimation needs, in our simulation we put 2 choices to the number of receiver microphones. Figure (5.8) shows the simulation of a target located in position (4, 7) using 4 microphones. As we can see from the figure, we get the exact position of the gun because Chan method is the optimum estimator for hyperbolic position location.

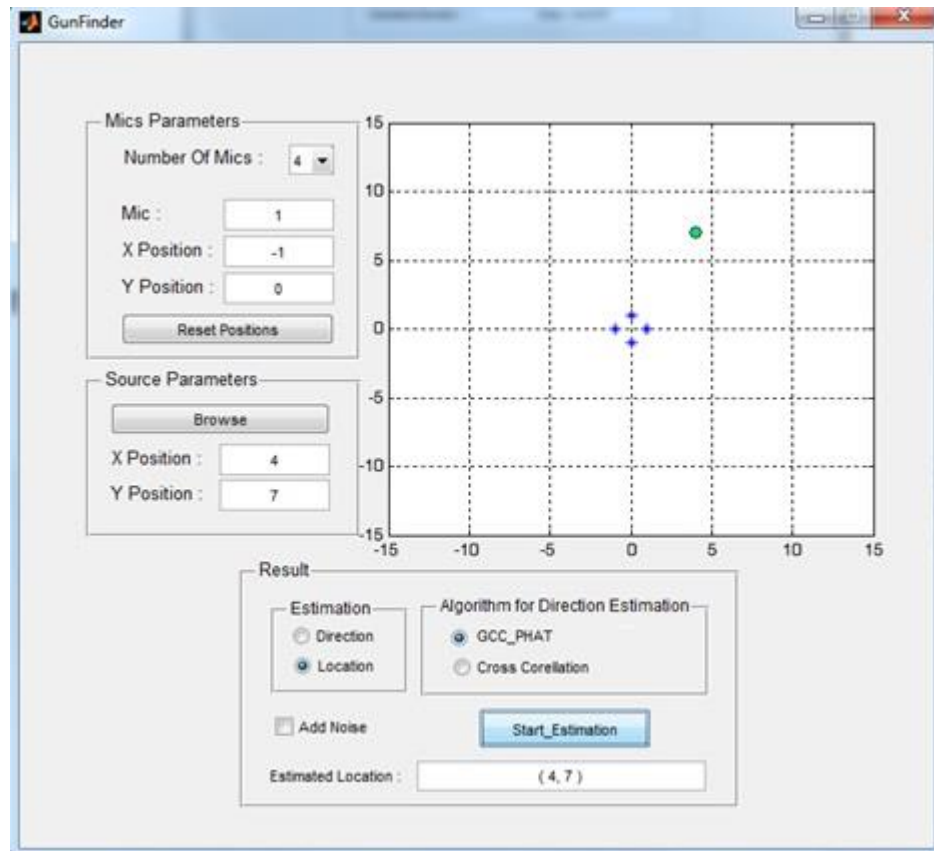


Figure : (5.6) Hyperbolic position location for Target in (4, 7), Mics in (1, 0), (-1, 0), (0, 1), (0, -1).

If we add uncertainty (noise) to the microphones positions (TDOA noise), we can see in Figure (5.9) that the result position location is not as the real one, so by adding more microphones Figure (5.10) we can get more information about the position of the gun, and get the exact location.

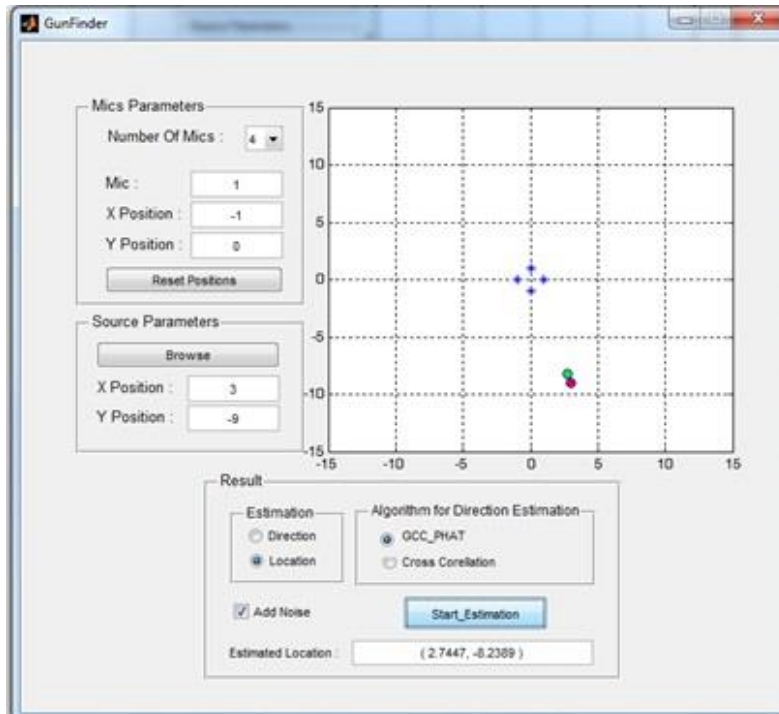


Figure : (5.7) Hyperbolic position location for Target in (4, 7) Mics in (1, 0), (-1, 0), (0, 1), (0, -1) with uncertainty in Mics locations.

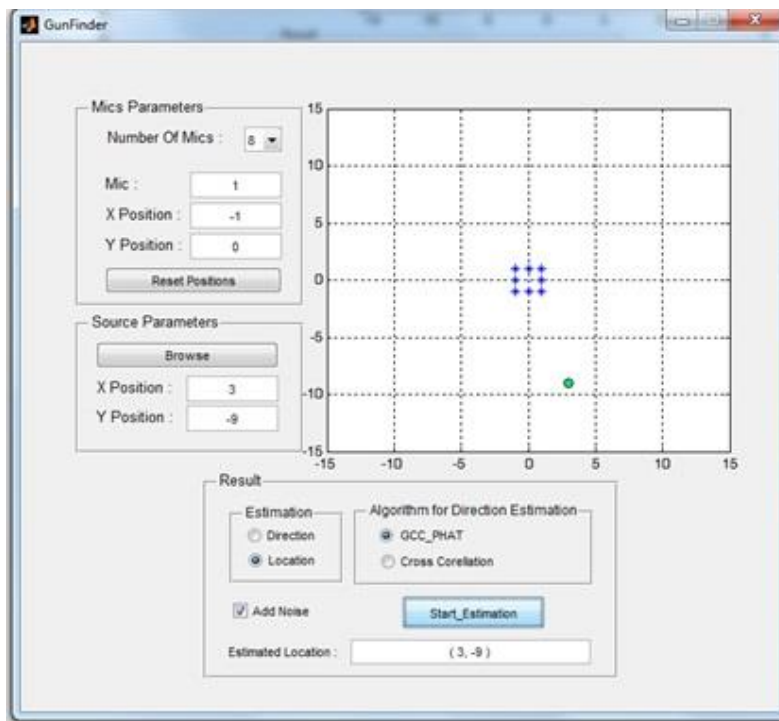


Figure : (5.8) Hyperbolic position location with 8 Mics, and uncertainty in Mics locations.

5.4. DOA Circuit:

The circuit begins with a pair of microphones separated by 7.5 cm. the microphones are connected to a microcontroller via an amplifier to amplify the wave sound. There are also 11 leds connected to the microcontroller to show the design output which is the DOA of gun sound. Figure (5.12) shows the schematic of the circuit.

5.4.1. Basic components:

➤ Microcontroller:

We use the Atmel AVR ATmega8, which is a low-power CMOS 8-bit microcontroller based on the AVR RISC architecture. By executing powerful instructions in a single clock cycle, the ATmega8 achieves throughputs approaching 1MIPS per MHz, allowing the system to optimize power consumption versus processing speed. Appendix A gives the features of Atmega8 Microcontroller.

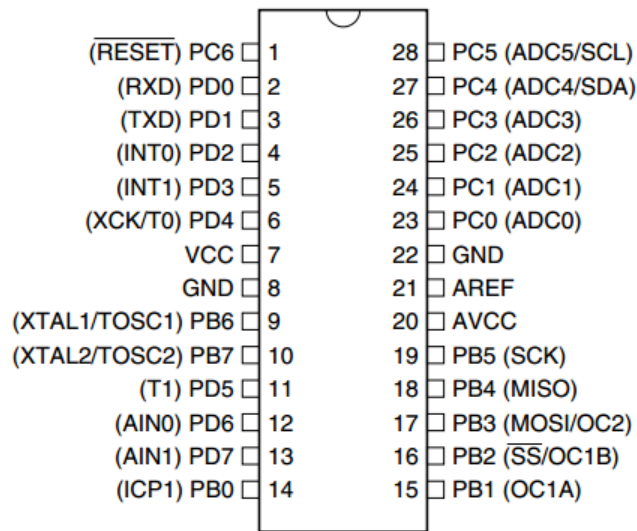


Figure : (5.9) Atmega8 microcontroller pin configuration.

➤ Sound wave amplifier:

The amplifier used is LM358, which is dual operational amplifier consist of two independent, high gain, internally frequency compensated operational amplifiers which were designed specifically to operate from a single power supply over a wide range of voltage. Figure (5.13) shows the internal block diagram of the amplifier, and the datasheet of the amplifier is shown in Appendix B.

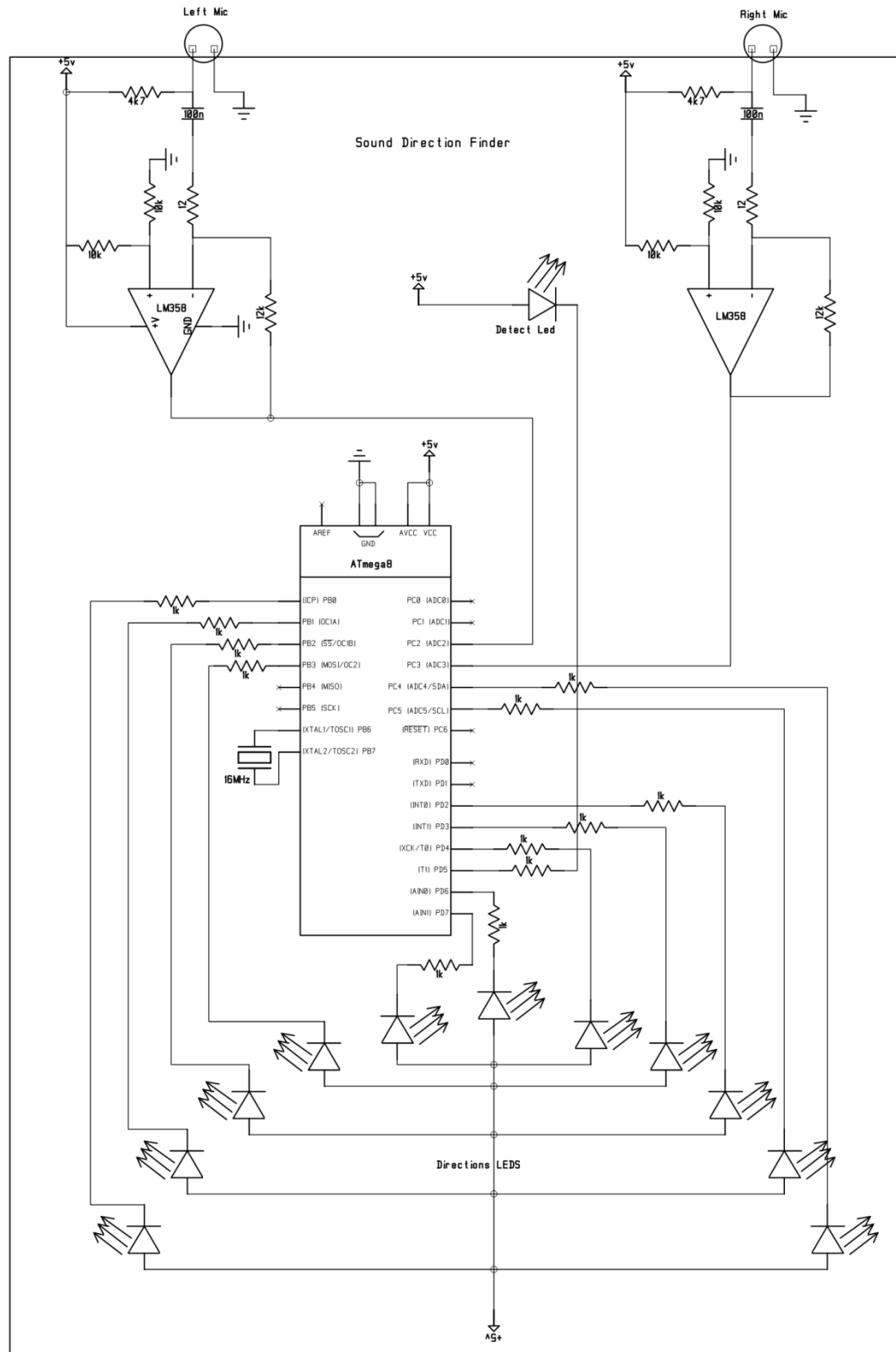


Figure : (5.10) Gun finder direction circuit schematic.

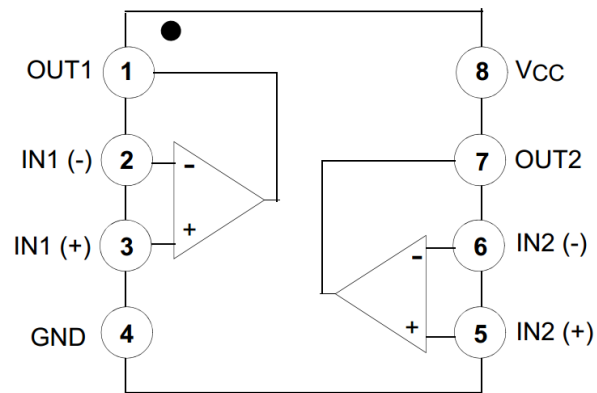


Figure : (5.11) LM358 internal block diagram.

5.4.2. System workflow:

The microphones capture the sound emitted from a gun, and then the acoustic signal is then amplified and converted via the microcontroller analog to digital converter (ADC) , the microcontroller calculates the cross correlation between the two received signals to find the delay between them, based on the delay value a leds lights to indicate the direction of arrival. Figure (5.14) shows the block diagram of the system.

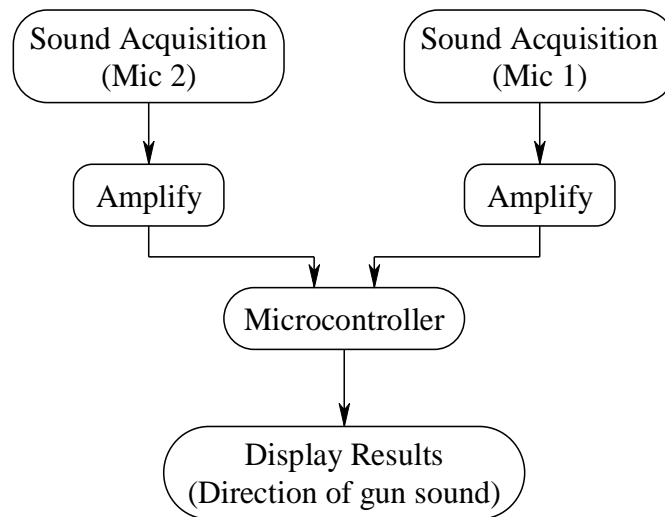


Figure : (5.12) Gun finder block diagram.

5.4.3 Microcontroller programming:

The next flowchart views the process of programming, which consists of the ADC converts the sound, cross correlation, and light the leds indicates the DOA of the sound. The program is included in Appendix C.

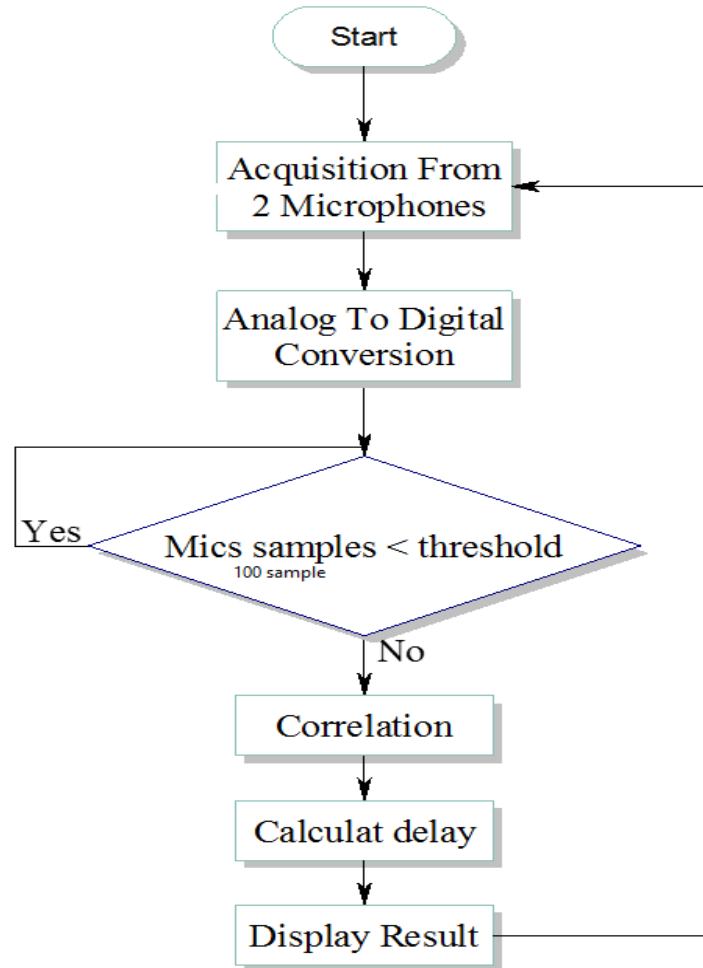


Figure : (5.13) flowchart of microcontroller program.

The acquisition is sampled via ADC converter with sample rate 30 KHz, we first check if the sound passed threshold (gun sound threshold). After a sample with a level more than threshold level acquired, we do cross correlation between 100 samples from microphone 1 and 100 samples from microphone 2. The result of the cross correlation determines how many samples are delayed between two signals. Finally we calculate the angle of arrival and display results on 11 leds indicates 11 directions. The led with the correct direction lights while others turned off. Figure (5.16) shows the acoustical direction finding (gun finder) circuit.

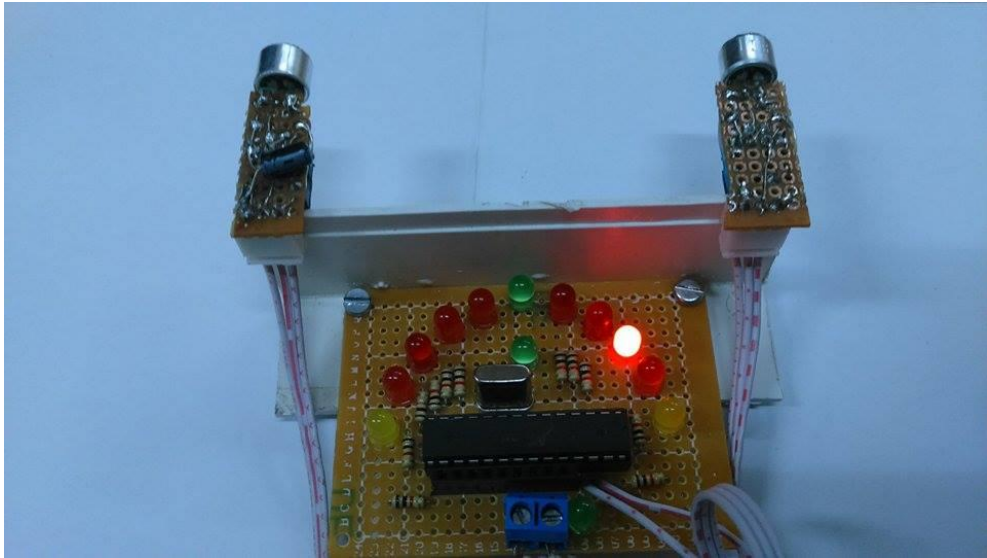


Figure : (5.14) acoustical direction finding (gun finder) circuit front.

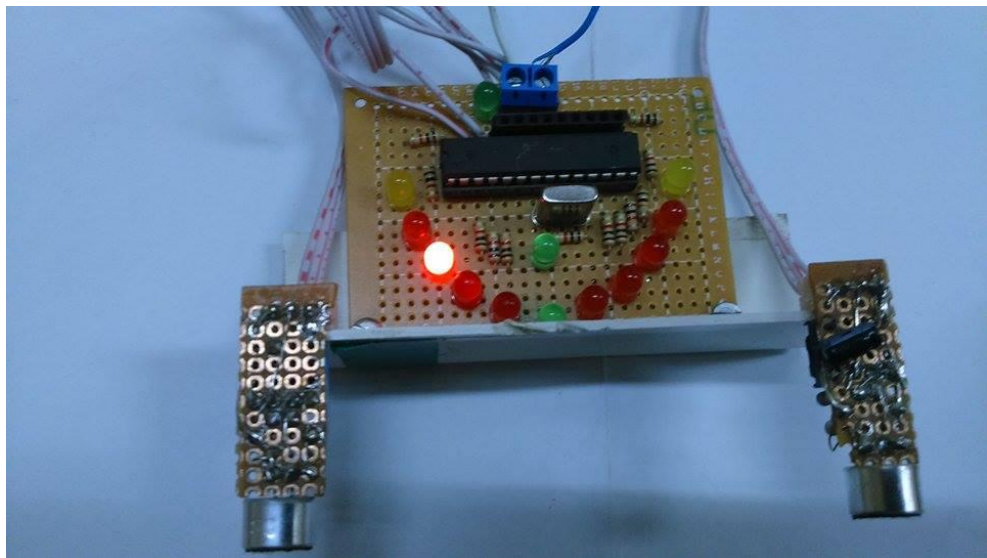


Figure : (5.15) acoustical direction finding (gun finder) circuit back.

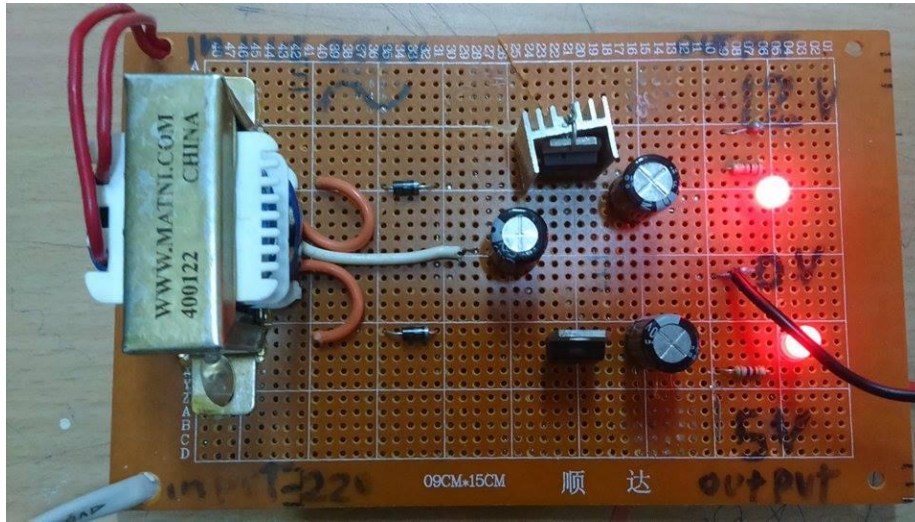


Figure : (5.16) Power supply circuit.

Conclusion:

The localization of an acoustic source in two different ways (position and direction) have been represented. Also implementation of the cross correlation and GCC-Phase Transform methods to estimate the direction of arrival using two microphones were considered .The principle of hyperbolic position location using implementation Chan method which is the optimum estimator to estimate location using four and eight microphones had discussed , the increase in the number of microphones to estimate the location leads to increase the accuracy, where the noise is existed. Finally a prototype of the circuit were tested to estimate the DOA of gun sound gave acceptable results .

Appendices

Appendix (A)

ATmega8 Microcontroller Datasheet

Features

- High-performance, Low-power Atmel® AVR® 8-bit Microcontroller
- Advanced RISC Architecture
 - 130 Powerful Instructions – Most Single-clock Cycle Execution
 - 32 x 8 General Purpose Working Registers
 - Fully Static Operation
 - Up to 16MIPS Throughput at 16MHz
 - On-chip 2-cycle Multiplier
- High Endurance Non-volatile Memory segments
 - 8Kbytes of In-System Self-programmable Flash program memory
 - 512Bytes EEPROM
 - 1Kbyte Internal SRAM
 - Write/Erase Cycles: 10,000 Flash/100,000 EEPROM
 - Data retention: 20 years at 85°C/100 years at 25°C⁽¹⁾
 - Optional Boot Code Section with Independent Lock Bits
 - In-System Programming by On-chip Boot Program
 - True Read-While-Write Operation
 - Programming Lock for Software Security
- Peripheral Features
 - Two 8-bit Timer/Counters with Separate Prescaler, one Compare Mode
 - One 16-bit Timer/Counter with Separate Prescaler, Compare Mode, and Capture Mode
 - Real Time Counter with Separate Oscillator
 - Three PWM Channels
 - 8-channel ADC in TQFP and QFN/MLF package
 - Eight Channels 10-bit Accuracy
 - 6-channel ADC in PDIP package
 - Six Channels 10-bit Accuracy
 - Byte-oriented Two-wire Serial Interface
 - Programmable Serial USART
 - Master/Slave SPI Serial Interface
 - Programmable Watchdog Timer with Separate On-chip Oscillator
 - On-chip Analog Comparator
- Special Microcontroller Features
 - Power-on Reset and Programmable Brown-out Detection
 - Internal Calibrated RC Oscillator
 - External and Internal Interrupt Sources
 - Five Sleep Modes: Idle, ADC Noise Reduction, Power-save, Power-down, and Standby
- I/O and Packages
 - 23 Programmable I/O Lines
 - 28-lead PDIP, 32-lead TQFP, and 32-pad QFN/MLF
- Operating Voltages
 - 2.7V - 5.5V (ATmega8L)
 - 4.5V - 5.5V (ATmega8)
- Speed Grades
 - 0 - 8MHz (ATmega8L)
 - 0 - 16MHz (ATmega8)
- Power Consumption at 4Mhz, 3V, 25°C
 - Active: 3.6mA
 - Idle Mode: 1.0mA
 - Power-down Mode: 0.5µA



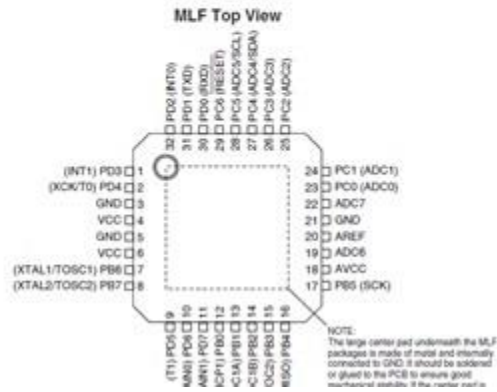
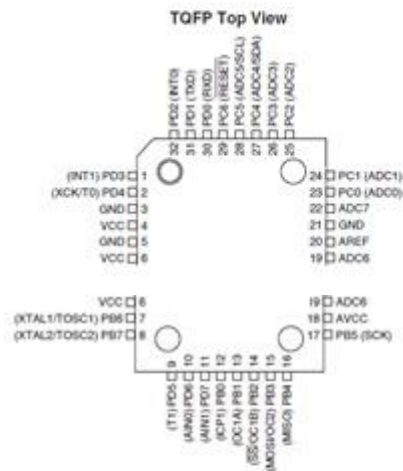
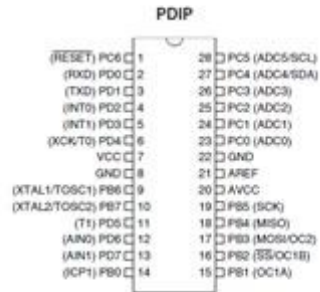
**8-bit Atmel with
8KBytes In-
System
Programmable
Flash**

**ATmega8
ATmega8L**

Rev. 2486AA-AVR-02/2013



Pin Configurations



Appendix (B)

LM358A Dual Operational Amplifier Datasheet

LM2904, LM358/LM358A, LM258/ LM258A

Dual Operational Amplifier

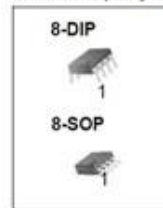
Features

- Internally Frequency Compensated for Unity Gain
- Large DC Voltage Gain: 100dB
- Wide Power Supply Range:
LM258/LM258A, LM358/LM358A: 3V-32V (or $\pm 1.5V \sim 16V$)
LM2904: 3V-26V (or $\pm 1.5V \sim 13V$)
- Input Common Mode Voltage Range Includes Ground
- Large Output Voltage Swing: 0V DC to $V_{CC} - 1.5V$ DC
- Power Drain Suitable for Battery Operation.

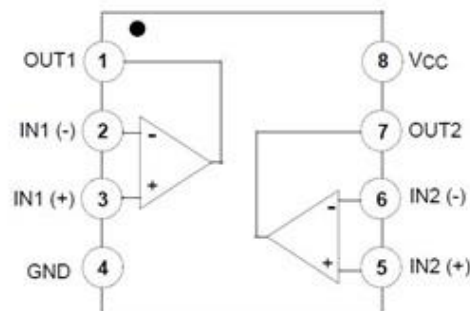
Description

The LM2904, LM358/LM358A, LM258/LM258A consist of two independent, high gain, internally frequency compensated operational amplifiers which were designed specifically to operate from a single power supply over a wide range of voltage. Operation from split power supplies is also possible and the low power supply current drain is independent of the magnitude of the power supply voltage. Application areas include transducer amplifier, DC gain

blocks and all the conventional OP-AMP circuits which now can be easily implemented in single power supply systems.



Internal Block Diagram



References:

- [1] “Handbook of Position Location: Theory, Practice, and Advances” Edited by Seyed (Reza) Zekavat and R. Michael Buehrer, IEEE Press, 2012.
- [2] Robert C. Maher, “MODELING AND SIGNAL PROCESSING OF ACOUSTIC GUNSHOT RECORDINGS”, IEEE, 2006 .
- [3] Robert C. Maher, “Acoustical Characterization of Gunshots”, 2007 .
- [4] Ashok Kumar Tellakula, “Acoustic Source Localization Using Time Delay Estimation”, Indian Institute of Science, 2007.

Smitha Paulose ,Elizabeth Sebastian ,Dr. Babu Paul, “Acoustic Source Localization”,
[5] International Journal of Advanced Research in Electrical, Electronics and Instrumentation Engineering, 2013.
- [6] JORDAN R. GRAVES, “AUDIO GUNSHOT DETECTION AND LOCALIZATION SYSTEMS: HISTORY, BASIC DESIGN, AND FUTURE POSSIBILITIES”, Northern Michigan University, 2010.

Derek Zong Thai, MatthewTrinkle, Ahmad Hashemi-Sakhtsari and Tim Pattison,
[7] “Speaker Localisation Using Time Difference of Arrival”, School of Electrical and Electronic Engineering The University of Adelaide, 2008 .
- [8] National Academy of Engineering, Engineering Challenges for the 21st Century, <http://www.engineeringchallenges.org/>, accessed 24 September 2011.
- [9] Dorsey, M., 2010, —Geolocation, next phase of the socialmedia revolution, focus of June 14 workshop at WPI, http://www.eurekaalert.org/pub_releases/2010-06/wpi-gnp060810.php